

Two-Dimensional Vibrating And Thermal Response of Skin Tissue To Different Types of Heat Sources Considering The Hyperbolic Heat Transfer Equation

Mina Ghanbari (✉ m.ghanbari@uut.ac.ir)

Urmia University of Technology

Ghader Rezazadeh

South Ural State University

Research Article

Keywords: hyperbolic heat conduction, thermoelastic, Skin tissue, Vibrating response, Galerkin method

Posted Date: August 31st, 2021

DOI: <https://doi.org/10.21203/rs.3.rs-835490/v1>

License:  This work is licensed under a Creative Commons Attribution 4.0 International License.

[Read Full License](#)

Two-dimensional vibrating and thermal response of skin tissue to different types of heat sources considering the hyperbolic heat transfer equation

Mina Ghanbari^{1*}, Ghader Rezazadeh²

¹*Mechanical Engineering Department, Urmia University of Technology, Urmia, Iran*

*Email: *m.ghanbari@urmia.ac.ir; Tel: +98 9144412381*

ORCID: [0000-0003-1315-9689](https://orcid.org/0000-0003-1315-9689)

²*Mechanical Engineering Department, Faculty of Engineering, Urmia University, Urmia, Iran & South Ural State University, Lenin prospect 76, Chelyabinsk, 454080, Russian Federation*

Email: g.rezazadeh@urmia.ac.ir

ORCID: [0000-0001-5243-3199](https://orcid.org/0000-0001-5243-3199)

Abstract

Laser-induced thermal therapy, due to its applications in various clinical treatments, has become an efficient alternative, especially for skin ablation. In this work, the two-dimensional thermomechanical response of skin tissue subjected to different types of thermal loading is investigated. Considering the thermoelastic coupling term, the two-dimensional differential equation of heat conduction in the skin tissue based on the Cattaneo–Vernotte heat conduction law is presented. The two-dimensional differential equation of the tissue displacement coupled with the two-dimensional hyperbolic heat conduction equation of tissue is solved simultaneously to analyze the thermal and mechanical response of the skin tissue. The existence of mixed complicated boundary conditions makes the problem so complex and intricate. The Galerkin-based reduced-order model has been utilized to solve the two-sided coupled differential equations of skin displacement and heat transfer with accompanying complicated boundary conditions. The effect of various types of heating sources such as thermal shock, single and repetitive pulses, repeating sequence stairs, ramp-type, and harmonic-type heating, on the thermomechanical response of the tissue is investigated. The temperature distribution in the tissue along the depth and radial direction is also presented. The transient temperature and displacement response of tissue considering different relaxation times are studied, and the results are discussed in detail.

Keywords: hyperbolic heat conduction; thermoelastic; Skin tissue; Vibrating response; Galerkin method

1. Introduction

In modern clinical treatments, thermal therapy is considered one of the most efficient existing alternatives. In thermal therapy, electromagnetic (EM) energy, ultrasonic waves, and other devices based on thermal conduction have been used as heating sources [1]. Thermal therapy aims to modify tissue temperature in a targeted region over time to compel a desired biological response. In the majority of designed thermotherapies, thermal therapy is delivered to a target

tissue volume with minimal impact on intervening or surrounding tissues. Thermal therapy emphasizes three techniques, namely, hyperthermia and thermal ablation. Hyperthermia can be categorized into long-term low-temperature hyperthermia in which the tissue temperature rises to 40-41°C for 6-72 hours and moderate-temperature hyperthermia in which tissue experiences 42-45°C for 15-60 minutes. In thermal ablation, also known as high-temperature hyperthermia, the tissue temperature rises to higher than 50°C for more than 6 minutes [1]. Laser-induced thermal therapy (LITT) plays a significant role in many oncology services as an alternative to conventional surgical interventions, especially for patients who are not good candidates for surgery. In other words, LITT is a percutaneous tumor-ablation procedure that delivers therapy due to the interstitially placed high-power lasers in the tumor. It delivers thermal therapy into the tumor cavity under MRI guidance, causing tumor ablation by compelling coagulation necrosis [2-3]. Reported studies show that it is also a very good option for the treatment of pediatric brain tumors [4] and small palpable invasive breast carcinomas [5]

Skin ablation utilizing energy-based devices has attracted increasing interest in the last few years. Skin ablation is an effective process not only for cosmetic purposes such as resurfacing, treating scars, or antiaging but also for therapeutic applications. In skin ablation, as the energy is divided into fractions, deep dermal penetration of the energy is achieved with minimal effect on the epidermis. It ensures a rapid recovery time compared with traditional ablative lasers [6].

Several developed ablative and non-ablative laser devices have been provided physicians with a wide palette of treatment options. In some studies, employing ablative lasers for the treatment of photoaged skin has shown efficacious results [7-8]. However, these painful procedures have several side effects, such as pigment alterations, infection, scarring, long-lasting erythema, and significant downtime. Ablative fractionated CO₂ or erbium:yag lasers are commonly applied techniques. The literature on nonablative fractional lasers (NAFLs) and ablative fractional lasers (AFLs) was reviewed by Tierney et al. [6]. This review supported the use of NAFL and AFL as an effective and safe treatment for photoaging. They showed that for the treatment of photoaging, fractionated resurfacing has important advantages over ablative laser resurfacing treatments. Bipolar radiofrequency is the other alternative method for the treatment of skin laxity, wrinkling with a low risk of scarring or persistent pigmentation [9]. It has been shown that bipolar fractionated RF treatment is considered a rapid wound healing response in which treatment intervals of at least 14 days should be recommended to allow performance of the remodeling process. In new technologies, high-intensity focused ultrasound (HIFU) is used to treat UV-induced hyperpigmentation. This method was commonly indicated for skin laxity. Vachiramon et al. reported the efficacy and safety of high-intensity focused ultrasound for UVB-induced hyperpigmentation in human subjects [10]. In the last few years, a new technology based on thermomechanical principles has been developed to present a novel treatment modality. Fractional treatment of aging skin with Tixel was reported by Elman et al.[11]. A novel device of Tixel, which is based on thermomechanical ablation technology, synthesizes temperature control and sophisticated motion. By applying Tixel as a novel technology, average treatment pain, downtime, and erythema clearance could be improved significantly. Therefore, Tixel could be used safely for nonablative and ablative resurfacing, such as scarring, the incidence of bleeding, or postinflammatory hyperpigmentation. Sintov and Hofmann assessed the effect of Tixel on the skin penetrance of three hydrophilic molecular models [12]. In the present work, no significant damage to the skin tissue or dermal coagulation was reported. The underlying wound-healing processes after skin ablation with thermomechanical ablation were investigated by Kokolakis et al.[13]. It was concluded that the wound-healing process after TMA is much faster, and the recovery time

minimizes significantly compared to other ablative techniques. The investigation of coagulation characteristics and ablation of a new CO laser and a high-power Tm: fiber laser were presented to assess their potential application for fractional ablation of the skin [14]. The use of a CO laser showed approximately two times larger coagulation zones than the CO₂ laser. The practicality of using noninvasive methods for objective skin assessment was evaluated following skin rejuvenation treatment [15]. After laser treatment, considerable improvement in facial skin aesthetics was recorded in brown spots, UV spots, and pores after 3 weeks, without significant changes in the tissue at the molecular level, as assessed by micro biopsy.

Thermal therapies and physiological studies such as hyperthermia, skin and tumor ablation, cryosurgery, frostbite, skin burns, and body thermal regulation and response to environmental conditions address the temperature rise in living tissues rising from the absorbed heat of the laser plus. Therefore, temperature distribution and the process of heating transfer and in living tissues play an important role in the effectiveness of thermal therapy methods. Presenting exact mathematical modeling of the heat transfer phenomenon is difficult due to the complexity of the nature of heat transfer in living tissue. Simplifications and assumptions must be made to make the problem obedient, in addition to capturing the essential features of the process. As the determination of temperature distribution in blood perfused tissue is very significant, heat transfer in biotissues has been studied numerously.

Several bioheat equations have been reported for modeling heat transfer in living tissue. The first bioheat equation was reported by Penne based on simplifying assumptions [16]. The assumptions of the presented model concerned four central factors: equilibrium site, blood perfusion, vascular architecture, and blood temperature. All prearteriole and postvenule heat transfers between blood and tissue were neglected. The flow of blood in the small capillaries was assumed to be isotropic. The effect of blood flow directionality and the local vascular geometry were also not considered in Penne's model. Despite the shortcomings of Penne's equation, it has enjoyed significant success in many applications, such as thermal stimulation of the whole body, cryosurgery, blood perfusion, hyperthermia therapy, and measurements. Chen and Holmes modified Penne's perfusion term, in which vascular geometry and blood flow directionality were taken into account [17]. Jiji et al. presented a three-temperature model for peripheral tissue where the temperature of arteries, veins, and tissue temperature was defined in the model for analyzing heat transfer [18]. Due to the difficulty of the three-temperature model, the three coupled deep layers were reduced to a single equation for the tissue temperature by applying simplifications [19]. The extracted differential equations for the bioheat equation in the discussed methods were all parabolic equations. They were obtained based on the classical Fourier's law, where heat pulses are supposed to propagate at infinite speed. An extended heat conduction model was introduced by Cattaneo [20] and Vernotte [21]. Applying Cattaneo-Vernotte (C-V) for extracting the differential heat conduction equation causes the partial differential equation to transform from parabolic to hyperbolic. In several types of research, the classical heat conduction equation has been modified to ensure finite speed pulse propagation to be compatible with physiological considerations and physical reality in a transient process [22]. To take into account microstructure interaction effects in the heat transfer process that were absent in the C-V model, Tzou introduced a generalized correlation between heat flux and temperature [23-24]. As the heat conduction model requires two-phase lags of the temperature gradient and heat flux, the heat transfer model is referenced as a dual-phase lag (DPL) model. In this model, the time delay parameter was a new indicator of bioheat efficiency in living tissue

Numerous studies have been reported on the use of the modified heat conduction equation in analyzing the temperature distribution in biotissue. Analytical estimation of the temperature and thermal damage in living tissue based on a hyperbolic bioheat model was investigated by Alzahrani and Abbas. [25]. The governing partial differential equation subject to laser irradiation was solved analytically in the Laplace domain. Comparing the analytical results with the existing experimental results showed the effectiveness of the mathematical model for biological heat transfer. In another work, the non-Fourier effect of laser-mediated thermal behaviors in biotissues was investigated [26]. Optical transmission and energy deposition were obtained by applying the Monte Carlo method. The dual-phase-lag model was applied and solved by employing a three-level finite difference method. Transient heating within skin tissue due to time-dependent thermal therapy was presented in the context of a memory-dependent heat transport law [27]. The heat transport equation for this problem concerning the memory-dependent derivative was formulated in the context of the Lord-Shulman (LS) model. The effects of time-dependent moving heat source velocity and the memory-dependent derivative on the thermal injuries and temperature of skin tissues were precisely investigated. Theoretical investigation of the temperature distribution in three-dimensional biological skin tissue was reported, in which the skin tissue was irradiated by multifiber lasers [28]. The results showed that the arrangement layout, spot size, and interval distance of the laser beams affected the obtained irradiated zone. Several types of research have been reported on the dual-phase-lag bioheat transfer model [29-31]. In one of the studies, to describe the interaction of a multipulse heat source and the skin, the dual-phase lag (DPL) bioheat transfer model and Henrique's burn assessment model were employed [32]. The influences of the biological parameters on the temperature distribution were discussed in detail. The thermomechanical behavior taking place in instantaneously heated skin tissue via an analytical approach was explored [33]. The generalized thermoelastic model involving a dual-phase-lag model of bioheat transfer was applied in a multilayer skin structure. Variable mechanical and thermal properties with spatial location and temperature were presented. Ezzat presented analytical thermomechanical responses of viscoelastic skin tissue [34]. The influences of variable thermal conductivity and volume material properties on the heat transfer of bioheat and the mechanical heat-induced response in a human skin plane were examined.

Although several works have been presented for modeling heat transfer in biotissues, the coupling thermoelastic term resulting from stretching or contracting of an elastic living tissue has not been considered in the heat transfer equation. Moreover, the vibration of elastic biotissue in exposure to a thermal source, which is important, especially in giving thermal shock to the tissue, is rarely studied [35-36]. In this work, a two-dimensional heat conduction equation of the skin tissue coupled with the two-dimensional equation governing displacement of the tissue was presented based on a modified Fourier law. Very complicated boundary conditions appear in this problem that should be satisfied. The two-side coupled equations of heat transfer and tissue movement are solved simultaneously to analyze the transient temperature and vibrating response of the tissue. The effect of several types of laser heat sources on the response of the tissue is investigated in more detail. The effect of thermoelastic terms on the temperature response of the tissue is also studied.

2. Governing equations

Figure 1 shows the biological skin tissue exposed to laser heating in cylindrical coordinates. When biological tissue receives laser irradiation, it will experience localized heating, optical energy absorption, and thermal expansion. The skin tissue on its surface irradiated by the laser is assumed to be a homogenous infinite elastic medium. By supposing an axisymmetric temperature distribution in the skin tissue, a two-dimensional distribution is considered along the r - and z -directions in this study. Tissue can also vibrate along the radial (r) and skin depth directions (z) by absorbing optical energy. The two-sided coupled governing equations of the two-dimensional heat conduction and two-dimensional vibration of the elastic media in cylindrical coordinates are extracted. They are solved simultaneously to obtain the temperature response of the biotissue exposed to laser heat. It is assumed that the radius of the laser beam is so small that the laser beam is assumed to be a localized heating source at $r=0$.

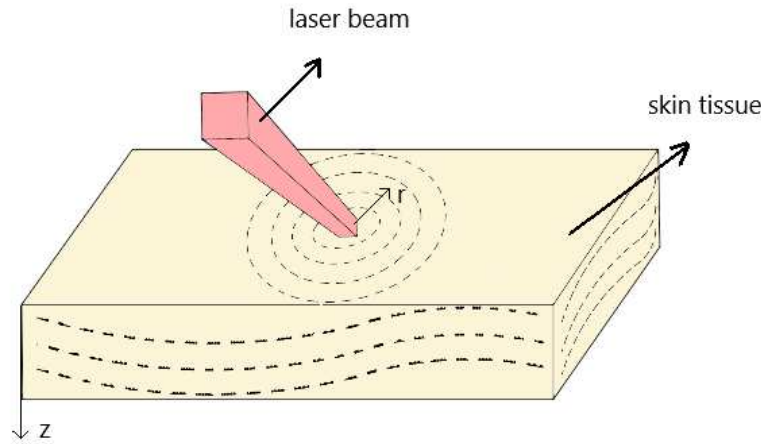


Figure 1 Thermoelastic vibration of the skin tissue in the presence of laser irradiation

2.1. Two-dimensional displacement equation of the tissue

The balanced equation of an elastic media is expressed as:

$$\mathfrak{S}_{ij,j} + \rho \mathfrak{b}_i = \rho \ddot{u}_i \quad (1)$$

where ρ is the tissue density, \mathfrak{b}_i is the body force per unit volume of the tissue, \mathfrak{S}_{ij} refers to stress components and u_i denotes the tissue displacement components. The balance equation in cylindrical coordinates in the r - and z -directions is expressed as:

$$\frac{\partial \mathfrak{S}_{rr}}{\partial r} + \frac{1}{r} \frac{\partial \mathfrak{S}_{r\theta}}{\partial \theta} + \frac{\partial \mathfrak{S}_{rz}}{\partial z} + \frac{1}{r} (\mathfrak{S}_{rr} - \mathfrak{S}_{\theta\theta}) + \rho \mathfrak{b}_r = \rho \frac{\partial^2 u}{\partial t^2} \quad (2)$$

$$\frac{\partial \mathfrak{S}_{rz}}{\partial r} + \frac{1}{r} \frac{\partial \mathfrak{S}_{\theta z}}{\partial \theta} + \frac{\partial \mathfrak{S}_{zz}}{\partial z} + \frac{1}{r} \mathfrak{S}_{rz} + \rho \mathfrak{b}_z = \rho \frac{\partial^2 v}{\partial t^2} \quad (3)$$

$$\frac{\partial \mathfrak{S}_{r\theta}}{\partial r} + \frac{1}{r} \frac{\partial \mathfrak{S}_{\theta\theta}}{\partial \theta} + \frac{\partial \mathfrak{S}_{\theta z}}{\partial z} + \frac{2}{r} \sigma_{r\theta} + \rho b_r = \rho \frac{\partial^2 w}{\partial t^2} \quad (4)$$

where u and v and w are displacement components of tissue displacement in the r -, z -, and θ -directions. The constitutive equation of an elastic media in the presence of the temperature distribution is defined as:

$$\mathfrak{S}_{ij} = \lambda \varepsilon_{kk} \delta_{ij} + 2\mu \varepsilon_{ij} - \mathfrak{B} \Delta T \delta_{ij} \quad (5)$$

In equation (4), δ_{ij} is the Kronecker delta, and T is the temperature. λ and μ are the Lamé constants related to the modulus of elasticity E and Poisson's ratio ν as:

$$\lambda = \frac{E\nu}{(1+\nu)(1-2\nu)}; \mu = \frac{E}{2(1+\nu)} \quad \square \text{where}$$

where, $\varepsilon_{ij} = \frac{1}{2}(u_{i,j} + u_{j,i})$ is the strain tensor. In relation (5) \mathfrak{B} is defined as:

$$\mathfrak{B} = \frac{E\alpha_T}{1-2\nu} \quad (7)$$

where α_T is the thermal expansion, E is the elasticity modulus of the tissue and ν is Poisson's ratio.

The components of the strain tensor in cylindrical coordinates are expressed as:

$$\begin{aligned} \varepsilon_{rr} &= \frac{\partial u}{\partial r}; \varepsilon_{\theta\theta} = \frac{1}{r} \left(\frac{\partial w}{\partial \theta} + u \right); \varepsilon_{zz} = \frac{\partial v}{\partial z}; \varepsilon_{r\theta} = \frac{1}{2} \left(\frac{1}{r} \frac{\partial u}{\partial \theta} + \frac{\partial w}{\partial r} - \frac{w}{r} \right); \\ \varepsilon_{\theta z} &= \frac{1}{2} \left(\frac{\partial w}{\partial z} + \frac{1}{r} \frac{\partial v}{\partial \theta} \right); \varepsilon_{zr} = \frac{1}{2} \left(\frac{\partial u}{\partial z} + \frac{\partial v}{\partial r} \right) \end{aligned} \quad (8)$$

Substituting strain components (8) into constitutive equation (4), the components of the stress tensor in cylindrical coordinates can be expressed as:

$$\begin{aligned} \mathfrak{S}_{rr} &= \lambda \left(\frac{\partial u}{\partial r} + \frac{1}{r} \left(\frac{\partial w}{\partial \theta} + u \right) + \frac{\partial v}{\partial z} \right) + 2\mu \frac{\partial u}{\partial r} - \mathfrak{B}(T(r, z, t) - T_0); \\ \mathfrak{S}_{r\theta} &= \mu \left(\frac{1}{r} \frac{\partial u}{\partial \theta} + \frac{\partial w}{\partial r} - \frac{w}{r} \right); \mathfrak{S}_{rz} = \mu \left(\frac{\partial u}{\partial z} + \frac{\partial v}{\partial r} \right); \\ \mathfrak{S}_{\theta\theta} &= \lambda \left(\frac{\partial u}{\partial r} + \frac{1}{r} \left(\frac{\partial w}{\partial \theta} + u \right) + \frac{\partial v}{\partial z} \right) + 2\mu \left(\frac{1}{r} \left(\frac{\partial w}{\partial \theta} + u \right) \right) - \mathfrak{B}(T(r, z, t) - T_0); \\ \mathfrak{S}_{\theta z} &= 2\mu \left(\frac{\partial w}{\partial z} + \frac{1}{r} \frac{\partial v}{\partial \theta} \right); \\ \mathfrak{S}_{zz} &= \lambda \left(\frac{\partial u}{\partial r} + \frac{1}{r} \left(\frac{\partial w}{\partial \theta} + u \right) + \frac{\partial v}{\partial z} \right) + 2\mu \left(\frac{\partial v}{\partial z} \right) - \mathfrak{B}(T(r, z, t) - T_0) \end{aligned} \quad (9)$$

T_0 is the reference temperature.

Substituting relation (9) into balance equations (2) and (3), the two-dimensional vibration of tissue in the r - and z -directions takes the following form:

$$\begin{aligned} (\lambda + 2\mu) \left(\frac{\partial^2 u}{\partial r^2} + \frac{1}{r} \left(\frac{\partial u}{\partial r} \right) - \left(\frac{u}{r^2} \right) \right) + \mu \left(\frac{\partial^2 u}{\partial z^2} \right) + (\lambda + \mu) \left(\frac{\partial^2 v}{\partial z \partial r} \right) - \mathfrak{B} \frac{\partial T}{\partial r} \\ = \rho \frac{\partial^2 u}{\partial t^2} + c \frac{\partial u}{\partial t} \end{aligned} \quad (10)$$

$$\begin{aligned}
& (\lambda + 2\mu) \left(\frac{\partial^2 v}{\partial z^2} \right) + \mu \left(\frac{\partial^2 v}{\partial r^2} + \frac{1}{r} \left(\frac{\partial v}{\partial r} \right) \right) + (\lambda + \mu) \left(\frac{\partial^2 u}{\partial r \partial z} + \frac{1}{r} \left(\frac{\partial u}{\partial z} \right) \right) \\
& - \mathfrak{B} \frac{\partial \mathcal{T}}{\partial z} = \rho \frac{\partial^2 v}{\partial t^2} + c \frac{\partial v}{\partial t}
\end{aligned} \tag{11}$$

2.1 Two-Dimensional hyperbolic heat transfer equation

Due to the importance of temperature distribution in biotissue in many medical therapies, such as brain tumor invasive breast carcinomas, hyperthermia, frostbite, and skin burns, predicting the accurate temperature response of biotissue to laser irradiation seems to be very important. Due to the complexity of the nature of heat transfer in living tissue, presenting a mathematical model for heat transfer needs logical simplifications. Several simplifications and assumptions must be made to make the problem tractable while capturing the essential features of the process. The local form of the energy balance equation in index notation is as follows:

$$\int_V (\dot{u} - \mathfrak{S}_{ij} \dot{\varepsilon}_{ij} - Q + q_{i,i}) dV = 0 \tag{12}$$

where σ is the stress, ε is the strain, u is the specific internal energy per unit volume, Q is known as the heat supply and denotes the rate at which heat per unit volume is produced by internal sources, and V is the volume. The rate at which heat is conducted into the body per unit area per unit time across the element of the surface is called the heat flux vector and is represented by the symbol q_i . Fourier's law states that the time rate of heat transfer through a material is proportional to the negative gradient of temperature and to the area at right angles through which the heat flows. It specifies a linear relationship between the temperature gradient and heat flux and is expressed as:

$$q_i = -k \mathcal{T}_{,i} \tag{13}$$

In equation (13), \mathcal{T} is temperature and k is the thermal conductivity $\left(\frac{W}{m.k} \right)$. In Fourier's law, the diffusion of heat gives rise to infinite speeds of heat propagation, which is incompatible with physical reality and physiological considerations in a transient process. Rapid thermal energy deposition is indicated in the medium, i.e., occurrence of any local temperature disturbance leads to an immediate perturbation in temperature at each point in the medium. Applying Fourier's law in the energy equation results in Pennes' bioheat equation, which is commonly used for modeling heat transfer in biological systems. Much attention has been devoted to modifying the classical heat conduction equation to ensure finite-speed pulse propagation. The generalized Fourier's law is called the Cattaneo–Vernotte heat conduction law. Utilizing it, the governing partial differential equation is transformed from parabolic to hyperbolic type. The constitutive equation of the Cattaneo–Vernotte model is characterized as follows:

$$q_i + \tau \dot{q}_i = k \mathcal{T}_{,i} \tag{14}$$

τ is the relaxation time, assumed to be a nonnegative constant.

Combining equations (12) and (14) results in the following heat conduction equation:

$$\mathcal{T}_{,ii} + Q + \tau \dot{Q} = \rho c \dot{\mathcal{T}} + \rho c \tau \ddot{\mathcal{T}} \tag{15}$$

In equation (15), c is the specific heat capacity of the tissue. The thermoelastic coupling term in the heat conduction equation is so small and usually neglected in practice [37]. It has been found to be important in many applications, such as thermal shocks [38-39], ultrafast laser heating in the

thermal processing of materials [40-41], modeling of the vibration of resonant microelectromechanical systems (MEMS) [42-43], and dynamic crack propagation [44]. Therefore, the thermoelastic effect should be taken into account in the mentioned application. By considering the thermoelastic effect in equation (14), it is modified to [39]:

$$k\mathcal{T}_{,ii} + Q + \tau\dot{Q} = \rho c\dot{\mathcal{T}} + \rho c\tau\ddot{\mathcal{T}} + \mathfrak{B}\mathcal{T}_0(\dot{\epsilon}_{kk} + \tau\ddot{\epsilon}_{kk}) \quad (16)$$

Q is the volumetric heat generated in the biotissue by blood perfusion, metabolism, and laser pulses as:

$$Q = Q_L + Q_B + Q_M \quad (17)$$

In equation (16), Q_L is the volumetric heat generated from a laser heat source [25]:

$$Q_L(z, t) = \mathfrak{f}_1(z)\mathfrak{f}_2(t) \quad (18)$$

where $\mathfrak{f}(z) = I_0\mu_a \left[\mathfrak{D}_1 e^{-\frac{e_1 z}{\mathfrak{h}}} - \mathfrak{D}_2 e^{-\frac{e_2 z}{\mathfrak{h}}} \right]$. I_0 is the laser intensity, μ_a is the absorption coefficient, and e_1, e_2, \mathfrak{D}_1 and \mathfrak{D}_2 are functions of diffuse reflectance (R_d) and are presented by Gardner et al. [25]. $\mathfrak{f}_2(t)$ is a time-dependent function and can be considered in any form as a repetitive pulse function, step function, harmonic function, and so on. \mathfrak{h} is the penetration depth and is characterized as follows [25]:

$$\mathfrak{h} = \frac{1}{\sqrt{3\mu_a(\mu_a + \mu_s(1 - \mathfrak{g}))}} \quad (19)$$

\mathfrak{g} is the anisotropy factor, and μ_s is the scattering coefficient.

Q_B in relation (16) is the volumetric heat generated by blood perfusion and is defined as:

$$Q_B = \rho_b c_b \omega_b (\mathcal{T}_b - \mathcal{T}) \quad (20)$$

where ρ_b and c_b are the density and the specific heat capacity of the blood, ω_b is the blood perfusion, and \mathcal{T}_b is the artery temperature. Q_M is the heat generated by the metabolic process due to various physiological processes occurring in the rest of the body and is neglected in this study. Substituting relations (8) and (17) in relation (16), the two-dimensional hyperbolic heat conduction equation is expressed as:

$$\begin{aligned} k \left(\frac{\partial^2 \mathcal{T}}{\partial r^2} + \frac{1}{r} \frac{\partial \mathcal{T}}{\partial r} + \frac{\partial^2 \mathcal{T}}{\partial z^2} \right) + \rho_b c_b \omega_b \mathcal{T}_b - \rho_b c_b \omega_b \mathcal{T} - \tau \rho_b c_b \omega_b \frac{\partial \mathcal{T}}{\partial t} \\ + Q_L(z, t) + \tau \dot{Q}_L(z, t) \\ = \rho c \frac{\partial \mathcal{T}}{\partial t} + \rho c \tau \frac{\partial^2 \mathcal{T}}{\partial t^2} + \mathfrak{B}\mathcal{T}_0 \left(\frac{\partial^2 u}{\partial t \partial r} + \frac{1}{r} \frac{\partial u}{\partial t} + \frac{\partial^2 v}{\partial t \partial z} \right) \\ + \mathfrak{B}\mathcal{T}_0 \tau \left(\frac{\partial^3 u}{\partial t^2 \partial r} + \frac{1}{r} \frac{\partial^2 u}{\partial t^2} + \frac{\partial^3 v}{\partial t^2 \partial z} \right) \end{aligned} \quad (21)$$

By considering the following nondimensional parameters:

$$\theta = \frac{\mathcal{T} - \mathcal{T}_0}{\mathcal{T}_0}; \theta_b = \frac{\mathcal{T}_b - \mathcal{T}_0}{\mathcal{T}_0}; \hat{r} = \frac{r}{\mathfrak{h}}; \hat{u} = \frac{u}{\mathfrak{h}}; \hat{t} = \frac{t}{t^*}; t^* = \frac{\mathfrak{h}^2}{\alpha}; \hat{z} = \frac{z}{\mathfrak{h}}; \hat{v} = \frac{v}{\mathfrak{h}}; \quad (22)$$

where $\alpha = k/\rho c$ (m^2/s) is the heat diffusivity of the tissue, and equations (19-21) take the following form:

$$\begin{aligned} \frac{\partial^2 \hat{u}}{\partial \hat{t}^2} - \mathfrak{M}_1 \frac{\partial \hat{u}}{\partial \hat{t}} - \mathfrak{M}_2 \left(\frac{\partial^2 \hat{u}}{\partial \hat{r}^2} \right) - \mathfrak{M}_2 \frac{1}{\hat{r}} \left(\frac{\partial \hat{u}}{\partial \hat{r}} \right) + \mathfrak{M}_2 \left(\frac{\hat{u}}{\hat{r}^2} \right) - \mathfrak{M}_3 \left(\frac{\partial^2 \hat{u}}{\partial \hat{z}^2} \right) \\ - \mathfrak{M}_4 \left(\frac{\partial^2 \hat{v}}{\partial \hat{z} \partial \hat{r}} \right) + \mathfrak{M}_5 \frac{\partial \theta}{\partial \hat{r}} = 0 \end{aligned} \quad (23)$$

$$\begin{aligned} \frac{\partial^2 \hat{v}}{\partial \hat{t}^2} - \mathfrak{M}_1 \frac{\partial \hat{v}}{\partial \hat{t}} - \mathfrak{M}_2 \left(\frac{\partial^2 \hat{v}}{\partial \hat{z}^2} \right) - \mathfrak{M}_3 \left(\frac{\partial^2 \hat{v}}{\partial \hat{r}^2} \right) - \mathfrak{M}_3 \left(\frac{1}{\hat{r}} \left(\frac{\partial \hat{v}}{\partial \hat{r}} \right) \right) - \mathfrak{M}_4 \left(\frac{\partial^2 \hat{u}}{\partial \hat{r} \partial \hat{z}} \right) \\ - \mathfrak{M}_4 \left(\frac{1}{\hat{r}} \left(\frac{\partial \hat{u}}{\partial \hat{z}} \right) \right) + \mathfrak{M}_5 \frac{\partial \theta}{\partial \hat{z}} = 0 \end{aligned} \quad (24)$$

$$\begin{aligned} \frac{\partial^2 \theta}{\partial \hat{t}^2} + \mathfrak{N}_1 \left(\frac{\partial^3 \hat{u}}{\partial \hat{t}^2 \partial \hat{r}} \right) + \mathfrak{N}_1 \left(\frac{1}{\hat{r}} \frac{\partial^2 \hat{u}}{\partial \hat{t}^2} \right) + \mathfrak{N}_1 \left(\frac{\partial^3 \hat{v}}{\partial \hat{t}^2 \partial \hat{z}} \right) + \mathfrak{N}_2 \frac{\partial \theta}{\partial \hat{t}} + \mathfrak{N}_3 \left(\frac{\partial^2 \hat{u}}{\partial \hat{t} \partial \hat{r}} \right) \\ + \mathfrak{N}_3 \left(\frac{1}{\hat{r}} \frac{\partial \hat{u}}{\partial \hat{t}} \right) + \mathfrak{N}_3 \left(\frac{\partial^2 \hat{v}}{\partial \hat{t} \partial \hat{z}} \right) - \mathfrak{N}_7 \left(\frac{\partial^2 \theta}{\partial \hat{r}^2} \right) - \mathfrak{N}_7 \left(\frac{1}{\hat{r}} \frac{\partial \theta}{\partial \hat{r}} \right) \\ - \mathfrak{N}_7 \left(\frac{\partial^2 \theta}{\partial \hat{z}^2} \right) - \varrho_4 \theta_b + \varrho_4 \theta - \mathfrak{N}_5 \hat{Q}_L(\hat{r}, \hat{z}, \hat{t}) - \mathfrak{N}_6 \hat{Q}_L(\hat{r}, \hat{z}, \hat{t}) = 0 \end{aligned} \quad (25)$$

with the following coefficients:

$$\begin{aligned} \mathfrak{M}_1 = \frac{c\delta^2}{\rho\alpha}; \mathfrak{M}_2 = \frac{(\lambda + 2\mu)\delta^2}{\rho\alpha^2}; \mathfrak{M}_3 = \frac{\mu\delta^2}{\rho\alpha^2}; \mathfrak{M}_4 = \frac{(\lambda + \mu)\delta^2}{\rho\alpha^2}; \mathfrak{M}_5 = \frac{\mathfrak{B}T_0\delta^2}{\rho\alpha^2}; \\ \mathfrak{N}_1 = \frac{\beta}{\rho c}; \mathfrak{N}_2 = \left(\frac{t^*}{\tau} + \frac{\rho_b c_b G_b t^*}{\rho c} \right); \mathfrak{N}_3 = \left(\frac{\beta t^*}{\rho c \tau} \right); \mathfrak{N}_4 = \frac{\rho_b c_b G_b t^{*2}}{\rho c \tau} \\ \mathfrak{N}_5 = \frac{t^{*2}}{\rho c \tau T_0}; \mathfrak{N}_6 = \frac{t^{*2}}{\rho c T_0}; \mathfrak{N}_7 = \frac{\delta^2}{\tau \alpha} \end{aligned} \quad (26)$$

In equation (25) the source term is expressed as:

$$\hat{Q}(\hat{z}, \hat{t}) = \mathfrak{f}_1(\bar{z}) \mathfrak{f}_2(\hat{t}) = \left(I_0 \mu_a \mathfrak{D}_1(e^{-e_1 \hat{z}}) - I_0 \mu_a \mathfrak{D}_2(e^{-e_2 \hat{z}}) \right) \mathfrak{f}_2(\hat{t}) \quad (27)$$

Nondimensional initial conditions for the displacement components of skin tissue and temperature are expressed as:

$$\theta(\hat{r}, \hat{z}, 0) = \dot{\theta}(\hat{r}, \hat{z}, 0) = \hat{u}(\hat{r}, \hat{z}, 0) = \dot{\hat{u}}(\hat{r}, \hat{z}, 0) = \hat{v}(\hat{r}, \hat{z}, 0) = \dot{\hat{v}}(\hat{r}, \hat{z}, 0) = 0; \quad (28)$$

Nondimensional boundary conditions for \bar{u}_r and \bar{u}_z in the r direction:

$$\lim_{\hat{r} \rightarrow \infty} \hat{u}(\hat{r}, \hat{z}, \hat{t}) = \hat{u}(0, \hat{z}, \hat{t}) = \lim_{\hat{r} \rightarrow \infty} \hat{v}(\hat{r}, \hat{z}, \hat{t}) = \left. \frac{\partial \hat{v}(\hat{r}, \hat{z}, \hat{t})}{\partial \hat{r}} \right|_{\hat{r}=0} = 0 \quad (29)$$

The nondimensional boundary conditions for \bar{u}_r and \bar{u}_z in the z direction are as follows:

$$\begin{aligned} \lim_{\hat{z} \rightarrow \infty} \hat{u}(\bar{r}, \hat{z}, \bar{t}) = \lim_{\hat{z} \rightarrow \infty} \hat{v}(\bar{r}, \hat{z}, \bar{t}) = 0; \\ \mathfrak{S}_{rz}|_{\hat{z}=0} = \left(\frac{\partial \hat{u}}{\partial \bar{z}} + \frac{\partial \hat{v}}{\partial \hat{r}} \right) \Big|_{\hat{z}=0} = 0; \end{aligned} \quad (30)$$

$$\mathfrak{S}_{zz}|_{\hat{z}=0} = \left\{ \left(\frac{\partial \hat{u}}{\partial \hat{r}} + \frac{\hat{u}}{\hat{r}} \right) + \mathfrak{M}_6 \left(\frac{\partial \hat{v}}{\partial \hat{z}} \right) - \mathfrak{M}_7 \theta(\hat{r}, \hat{z}, \hat{t}) \right\} \Big|_{\hat{z}=0} = 0 \quad (31)$$

where $\mathfrak{M}_6 = \frac{(\lambda+2\mu)}{\lambda}$; $\mathfrak{M}_7 = \frac{\mathfrak{B}\mathcal{T}_0}{\lambda}$. Nondimensional boundary conditions for the temperature along the r and z directions are:

$$\lim_{\hat{r} \rightarrow \infty} \theta(\hat{r}, \hat{z}, \hat{t}) = \lim_{\hat{z} \rightarrow \infty} \theta(\hat{r}, \hat{z}, \hat{t}) = \frac{\partial \theta(\hat{r}, \hat{z}, \hat{t})}{\partial \hat{r}} \Big|_{\hat{r}=0} = 0; \frac{\partial \theta(\hat{r}, \hat{z}, \hat{t})}{\partial \hat{z}} \Big|_{\hat{z}=0} \cong 0 \quad (32)$$

3. Numerical Method

In this study, the Galerkin-based reduced-order model was utilized to solve the coupled two-dimensional partial differential equations of hyperbolic heat transfer and vibrating biotissue equations. Utilizing the Galerkin method, a continuous operator problem, such as a differential equation, commonly in a weak formulation, is converted to a discrete problem. It is done by applying linear constraints determined by finite sets of basic functions. This method is the equivalent of applying the method of variation of parameters to function space by converting the equation to a weak formulation. It is based on the weak formulation of an equation and limits the possible solutions to a smaller space than the original one, which can be solved more easily. A linear combination of a set of prescribed basis or shape functions is considered for the unknown function. Satisfying the boundary conditions of the problem is dependent on selecting proper shape functions. The accuracy of the solutions depends significantly on the number and type of shape functions.

In this work, complex boundary conditions, especially those related to stresses on the surface of the tissue, appear. To satisfy the complicated boundary conditions, the following approximate solutions are considered for equations (23)-(25).

$$\hat{u}(\hat{r}, \hat{z}, \hat{t}) = \sum_{i=1}^n \sum_{j=1}^m \mathfrak{Y}_i(\hat{r}) \mathfrak{F}_j(\hat{z}) q_{ij}(\hat{t}) + \sum_{i=1}^n \sum_{j=1}^m \mathcal{A}_i \mathfrak{Y}_i(\hat{r}) \mathfrak{F}_j^*(\hat{z}) q_{ij}(\hat{t}) \quad (33)$$

$$\hat{v}(\hat{r}, \hat{z}, \hat{t}) = \sum_{p=1}^a \sum_{q=1}^b \mathfrak{R}_p(\hat{r}) \mathfrak{H}_q(\hat{z}) \mathfrak{P}_{pq}(\hat{t}) + \sum_{i=1}^n \sum_{j=1}^m \mathcal{B}_i \mathfrak{R}_p(\hat{r}) \mathfrak{H}_j^*(\hat{z}) \mathfrak{P}_{pq}(\hat{t}) \quad (34)$$

$$\theta(\hat{r}, \hat{z}, \hat{t}) = \sum_{k=1}^u \sum_{d=1}^s \mathfrak{T}_k(\hat{r}) \mathfrak{L}_d(\hat{z}) s_{kd}(\hat{t}) \quad (35)$$

\mathcal{A}_i and \mathcal{B}_i are time dependant functions and are selected to satisfy the boundary conditions (31). The approximate solutions (33), (34), and (35) are substituted into equations (23), (24), and (25) and the boundary conditions (31) as:

$$\begin{aligned}
\hat{t}) - \mathfrak{M}_1 \sum_{i=1}^n \sum_{j=1}^m \mathfrak{Y}_i(\hat{r}) (\mathfrak{F}_j(\hat{z}) + \mathcal{A}_i \mathfrak{F}_j^*(\hat{z})) \dot{q}_{ij}(\hat{t}) \\
- \mathfrak{M}_2 \sum_{i=1}^n \sum_{j=1}^m \left(\mathfrak{Y}_i'(\hat{r}) + \frac{1}{\hat{r}} \mathfrak{Y}_i(\hat{r}) - \frac{1}{\hat{r}^2} \mathfrak{Y}_i(\hat{r}) \right) (\mathfrak{F}_j(\hat{z}) + \mathcal{A}_i \mathfrak{F}_j^*(\hat{z})) \\
- \mathfrak{M}_3 \left(\mathfrak{Y}_i(\hat{r}) (\mathfrak{F}_j''(\hat{z}) + \mathcal{A}_i \mathfrak{F}_j^{*'}(\hat{z})) \right) q_{ij}(\hat{t}) \\
- \mathfrak{M}_4 \sum_{p=1}^a \sum_{q=1}^b \mathfrak{R}_p'(\hat{r}) (\mathfrak{S}_q(\hat{z}) + \mathcal{B} \mathfrak{S}_q^*(\hat{z})) \dot{p}_{pq}(\hat{t}) \\
+ \mathfrak{M}_5 \sum_{k=1}^u \sum_{d=1}^s \mathfrak{S}_k(\hat{r}) \mathfrak{Q}_d(\hat{z}) \delta_{kd}(\hat{t}) = \varepsilon_1
\end{aligned} \tag{36}$$

$$\begin{aligned}
\sum_{p=1}^a \sum_{q=1}^b \mathfrak{R}_p(\hat{r}) (\mathfrak{S}_q(\bar{z}) + B_i \mathfrak{S}_q^*(\hat{z})) \ddot{p}_{pq}(\hat{t}) \\
- \mathfrak{M}_1 \sum_{p=1}^a \sum_{q=1}^b \mathfrak{R}_p(\hat{r}) (\mathfrak{S}_q(\bar{z}) + B_i \mathfrak{S}_q^*(\hat{z})) \dot{p}_{pq}(\hat{t}) \\
- \mathfrak{M}_2 \sum_{p=1}^a \sum_{q=1}^b \left(\mathfrak{R}_p(\hat{r}) (\mathfrak{S}_q''(\bar{z}) + B_i \mathfrak{S}_q^{*''}(\hat{z})) \right) \\
- \mathfrak{M}_2 \left(\mathfrak{R}_p'(\hat{r}) + \frac{1}{\hat{r}} \mathfrak{R}_p(\hat{r}) \right) (\mathfrak{S}_q(\hat{z}) + B_i \mathfrak{S}_q^*(\hat{z})) \dot{p}_{pq}(\hat{t}) \\
- \mathfrak{M}_4 \sum_{i=1}^n \sum_{j=1}^m \left(\mathfrak{Y}_i(\hat{r}) + \frac{1}{\hat{r}} \mathfrak{Y}_i(\hat{r}) \right) (\mathfrak{F}_j(\hat{z}) + \mathfrak{F}_j'(\hat{z})) q_{ij}(\hat{t}) \\
+ \mathfrak{M}_5 \sum_{k=1}^u \sum_{d=1}^s \mathfrak{S}_k(\hat{r}) \mathfrak{Q}_d(\hat{z}) \delta_{kd}(\hat{t}) = \varepsilon_2
\end{aligned} \tag{37}$$

$$\begin{aligned}
& \sum_{k=1}^u \sum_{d=1}^s \mathfrak{F}_k(\hat{r}) \mathfrak{L}_d(\hat{z}) \ddot{s}_{cd}(\hat{t}) \\
& + \mathfrak{N}_1 \sum_{i=1}^n \sum_{j=1}^m \left(\left(\mathfrak{Y}_i(\hat{r}) + \frac{1}{\hat{r}} \mathfrak{Y}_i(\bar{r}) \right) \left(\mathfrak{F}_j(\hat{z}) + A_i \mathfrak{F}_j^*(\hat{z}) \right) \right) \ddot{q}_{ij}(\hat{t}) \\
& + \mathfrak{N}_1 \sum_{p=1}^a \sum_{q=1}^b \mathfrak{R}_p(\hat{r}) \left(\mathfrak{S}_q(\hat{r}) + B_i \mathfrak{S}_q^*(\hat{z}) \right) \ddot{p}_{ab}(\hat{t}) \\
& + \mathfrak{N}_2 \sum_{k=1}^u \sum_{d=1}^s \mathfrak{F}_k(\hat{r}) \Phi_d(\hat{z}) \dot{s}_{kd}(\hat{t}) \\
& + \mathfrak{N}_3 \sum_{i=1}^n \sum_{j=1}^m \left(\left(\mathfrak{Y}_i(\hat{r}) + \frac{1}{\hat{r}} \mathfrak{Y}_i(\bar{r}) \right) \left(\mathfrak{F}_j(\hat{z}) + A_i \mathfrak{F}_j^*(\hat{z}) \right) \right) \dot{q}_{ij}(\hat{t}) \\
& + \mathfrak{N}_3 \sum_{p=1}^a \sum_{q=1}^b \mathfrak{R}_p(\hat{r}) \left(\mathfrak{S}_q(\bar{r}) + B_i \mathfrak{S}_q^*(\hat{z}) \right) \dot{p}_{pq}(\hat{t}) \\
& - \sum_{k=1}^u \sum_{d=1}^s \left(\left(\left(\mathfrak{S}_k'(\hat{r}) + \frac{1}{\hat{r}} \mathfrak{S}_k'(\bar{r}) \right) - (\mathfrak{N}_4 \mathfrak{S}_k(\bar{r})) \right) \mathfrak{L}_d(\hat{z}) \right. \\
& \left. + \mathfrak{S}_k(\hat{r}) \mathfrak{L}_d'(\hat{z}) \right) s_{kd}(\hat{t}) - \mathfrak{N}_4 \theta_b - \mathfrak{N}_5 \hat{\mathcal{Q}}_{\mathcal{L}}(\hat{r}, \hat{z}, \hat{t}) - \mathfrak{N}_6 \dot{\hat{\mathcal{Q}}}_{\mathcal{L}}(\hat{r}, \hat{z}, \hat{t}) \\
& = \varepsilon_3
\end{aligned} \tag{38}$$

$$\begin{aligned}
& \sum_{i=1}^n \sum_{j=1}^m \mathfrak{Y}_i(\hat{r}) \left(\mathfrak{F}_j(0) + A_i \mathfrak{F}_j^*(0) \right) q_{ij}(\hat{t}) \\
& + \sum_{p=1}^a \sum_{q=1}^b \mathfrak{R}_p(\hat{r}) \left(\mathfrak{S}_q(0) + B_i \mathfrak{S}_q^*(0) \right) \chi_{pq}(\hat{t}) = \varepsilon_4
\end{aligned} \tag{39}$$

$$\begin{aligned}
& \sum_{i=1}^n \sum_{j=1}^m \left(\left(\mathfrak{Y}_i(\hat{r}) + \frac{1}{\hat{r}} \mathfrak{Y}_i(\hat{r}) \right) \left(\mathfrak{F}_j(0) + A_i \mathfrak{F}_j^*(0) \right) \right) q_{ij}(\hat{t}) \\
& + \Upsilon_5 \sum_{p=1}^a \sum_{q=1}^b \mathfrak{R}_p(\hat{r}) \left(\mathfrak{S}_q(0) + B_i \mathfrak{S}_q^*(0) \right) \chi_{pq}(\hat{t}) \\
& - \Upsilon_6 \sum_{k=1}^u \sum_{d=1}^s \mathfrak{F}_k(\hat{r}) \mathfrak{L}_d(0) \xi_{kd}(\hat{t}) = \varepsilon_5
\end{aligned} \tag{40}$$

Applying the following Galerkin integrals yields:

$$\int_0^\infty \int_0^\infty \varepsilon_1 \mathfrak{Y}_e(\hat{r}) \mathfrak{F}_f(\hat{z}) d\hat{r} d\hat{z} = 0 \quad e = 1, 2, \dots, n, \quad f = 1, 2, \dots, m \tag{41}$$

$$\int_0^\infty \int_0^\infty \varepsilon_2 \mathfrak{R}_g(\bar{r}) \mathfrak{S}_h(\bar{z}) d\hat{r} d\hat{z} = 0 \quad g = 1, 2, \dots, p, \quad h = 1, 2, \dots, q \quad (42)$$

$$\int_0^\infty \int_0^\infty \varepsilon_3 \mathfrak{S}_c(\hat{r}) \mathfrak{Q}_l(\bar{z}) d\hat{r} d\hat{z} = 0 \quad c = 1, 2, \dots, u, \quad l = 1, 2, \dots, s \quad (43)$$

$$\int_0^\infty \varepsilon_4 \mathfrak{Y}_e(\hat{r}) d\hat{r} = 0 \quad e = 1, 2, 3, \dots, n \quad (44)$$

$$\int_0^\infty \varepsilon_5 \mathfrak{R}_g(\hat{r}) d\hat{r} = 0 \quad g = 1, 2, 3, \dots, a \quad (45)$$

The following equations are obtained:

$$\begin{aligned} & \sum_{i=1}^n \sum_{j=1}^m M_{ei}^{(1)} (M_{fj}^{(2)} + A_i M_{fj}^{(3)}) \ddot{q}_{ij}(\hat{t}) - \sum_{i=1}^n \sum_{j=1}^m C_{ei}^{(1)} (C_{fj}^{(2)} + A_i C_{fj}^{(3)}) \ddot{q}_{ij}(\hat{t}) \\ & - \sum_{i=1}^n \sum_{j=1}^m \left(K_{ei}^{(1)} (K_{fj}^{(2)} + A_i K_{fj}^{(3)}) + K_{ei}^{(4)} (K_{fj}^{(5)} + A_i K_{fj}^{(6)}) \right) q_{ij}(\hat{t}) \\ & - \sum_{p=1}^a \sum_{q=1}^b E_{ep}^{(1)} (E_{fq}^{(2)} + B_i E_{fq}^{(3)}) \mathcal{P}_{pq}(\hat{t}) + \sum_{k=1}^u \sum_{d=1}^s F_{ek}^{(1)} F_{fd}^{(2)} \mathcal{S}_{kd}(\hat{t}) \\ & = 0 \end{aligned} \quad (46)$$

$$\begin{aligned} & \sum_{p=1}^a \sum_{q=1}^b M_{gp}^{(4)} (M_{hq}^{(5)} + B_i M_{hq}^{(6)}) \ddot{\mathcal{P}}_{pq}(\hat{t}) - \sum_{p=1}^a \sum_{q=1}^b C_{gp}^{(4)} (C_{hq}^{(5)} + B_i C_{hq}^{(6)}) \ddot{\mathcal{P}}_{pq}(\hat{t}) \\ & - \sum_{p=1}^a \sum_{q=1}^b \left(E_{gp}^{(4)} (E_{hq}^{(5)} + B_i E_{hq}^{(6)}) + E_{gp}^{(7)} (E_{gp}^{(8)} + B_i E_{gp}^{(9)}) \right) \mathcal{P}_{pq}(\hat{t}) \\ & - \sum_{i=1}^n \sum_{j=1}^m \left(K_{gi}^{(7)} (K_{hj}^{(8)} + A_i K_{hj}^{(9)}) \right) q_{ij}(\hat{t}) + \sum_{k=1}^u \sum_{d=1}^s (F_{gk}^{(3)} F_{hd}^{(4)}) \mathcal{S}_{cd}(\hat{t}) \\ & = 0 \end{aligned} \quad (47)$$

$$\begin{aligned}
& \sum_{k=1}^u \sum_{d=1}^s (M_{ck}^{(7)} M_{ld}^{(8)}) \mathfrak{S}_{kd}(\hat{t}) \\
& + \sum_{i=1}^n \sum_{j=1}^m M_{ci}^{(9)} (M_{lj}^{(10)} + A_i M_{lj}^{(11)}) \mathfrak{Q}_{ij}(\hat{t}) \\
& + \sum_{p=1}^a \sum_{q=1}^b M_{cp}^{(12)} (M_{lq}^{(13)} + B_i M_{lq}^{(14)}) \mathfrak{P}_{pq}(\hat{t}) \\
& + \sum_{k=1}^u \sum_{d=1}^s (C_{ck}^{(7)} C_{ld}^{(8)}) \mathfrak{S}_{kd}(\hat{t}) \\
& + \sum_{i=1}^n \sum_{j=1}^m C_{ci}^{(9)} (C_{lj}^{(10)} + A_i C_{lj}^{(11)}) \mathfrak{Q}_{ij}(\hat{t}) \\
& + \sum_{p=1}^a \sum_{q=1}^b C_{cp}^{(12)} (C_{lq}^{(13)} + B_i C_{lq}^{(14)}) \mathfrak{P}_{pq}(\hat{t}) \\
& - \sum_{k=1}^u \sum_{d=1}^s (F_{ck}^{(5)} F_{ld}^{(6)} + F_{ck}^{(7)} F_{ld}^{(8)}) \mathfrak{S}_{kd}(\hat{t}) - P_{cl}^{(1)} - P_{cl}^{(2)}(\hat{t}) - P_{cl}^{(3)}(\hat{t}) \\
& = 0
\end{aligned} \tag{48}$$

$$\begin{aligned}
& \sum_{i=1}^n \sum_{j=1}^m K_{ei}^{(10)} (K_j^{(11)} + A_i K_j^{(12)}) \mathfrak{Q}_{ij}(\hat{t}) + \sum_{p=1}^a \sum_{q=1}^b E_{ep}^{(10)} (E_q^{(11)} + B_i E_q^{(12)}) \mathfrak{P}_{pq}(\hat{t}) \\
& = 0
\end{aligned} \tag{49}$$

$$\begin{aligned}
& \sum_{i=1}^n \sum_{j=1}^m K_{gi}^{(13)} (K_j^{(14)} + A_i K_j^{(15)}) \mathfrak{Q}_{ij}(\hat{t}) \\
& + \sum_{p=1}^a \sum_{q=1}^b E_{gp}^{(13)} (E_q^{(14)} + B_i E_q^{(15)}) E_q^{(15)} \mathfrak{P}_{pq}(\hat{t}) \\
& - \sum_{k=1}^u \sum_{d=1}^s F_{gk}^{(9)} F_d^{(10)} \mathfrak{S}_{kd}(\hat{t}) = 0
\end{aligned} \tag{50}$$

With the following coefficients:

$$\begin{aligned}
M_{ei}^{(1)} &= \int_0^\infty \mathfrak{Y}_e(\hat{r}) \mathfrak{Y}_i(\hat{r}) d\hat{r}; M_{fj}^{(2)} = \int_0^\infty \mathfrak{F}_f(\hat{z}) \mathfrak{F}_j(\hat{z}) d\hat{z}; M_{fj}^{(3)} = \int_0^\infty \mathfrak{F}_f(\hat{z}) \mathfrak{F}_j^*(\hat{z}) d\hat{z}; \\
C_{ei}^{(1)} &= \mathfrak{M}_1 \int_0^\infty \mathfrak{Y}_e(\hat{r}) \mathfrak{Y}_i(\hat{r}) d\hat{r}; C_{fj}^{(2)} = \int_0^\infty \mathfrak{F}_f(\hat{z}) \mathfrak{F}_j(\hat{z}) d\hat{z}; C_{fj}^{(3)} = \int_0^\infty \mathfrak{F}_f(\hat{z}) \mathfrak{F}_j^*(\hat{z}) d\hat{z}; \\
K_{ei}^{(1)} &= \mathfrak{M}_2 \int_0^\infty \mathfrak{Y}_e(\hat{r}) \left(\mathfrak{Y}_i(\hat{r}) + \frac{1}{\hat{r}} \mathfrak{Y}_i(\hat{r}) - \frac{1}{\hat{r}^2} \mathfrak{Y}_i(\hat{r}) \right) d\hat{r}; K_{fj}^{(2)} = \int_0^\infty \mathfrak{F}_f(\hat{z}) \mathfrak{F}_j(\hat{z}) d\hat{z};
\end{aligned}$$

$$\begin{aligned}
K_{fj}^{(3)} &= \int_0^\infty \mathfrak{F}_f(\hat{z}) \mathfrak{F}_j^*(\hat{z}) d\hat{z}; K_{ei}^{(4)} = \mathfrak{W}_3 \int_0^\infty \mathfrak{Y}_e(\hat{r}) \mathfrak{Y}_i(\hat{r}) d\hat{r}; K_{fj}^{(5)} = \int_0^\infty \mathfrak{F}_f(\hat{z}) \mathfrak{F}_j''(\hat{z}) d\hat{z} \\
K_{fj}^{(6)} &= \int_0^\infty \mathfrak{F}_f(\hat{z}) \mathfrak{F}_j''(\hat{z}) d\hat{z}; E_{ep}^{(1)} = \mathfrak{W}_4 \int_0^\infty \mathfrak{Y}_e(\hat{r}) \mathfrak{R}_p(\hat{r}) d\hat{r}; E_{fq}^{(2)} = \int_0^\infty \mathfrak{F}_f(\hat{z}) \mathfrak{S}_q(\hat{z}) d\hat{z} \\
E_{fq}^{(3)} &= \int_0^\infty \mathfrak{F}_f(\hat{z}) \mathfrak{S}_q^*(\hat{z}) d\hat{z}; F_{ek}^{(1)} = \mathfrak{W}_5 \int_0^\infty \mathfrak{Y}_e(\hat{r}) \mathfrak{S}_k(\hat{r}) d\hat{r}; F_{fd}^{(2)} = \int_0^\infty \mathfrak{F}_f(\hat{z}) \Phi_d(\hat{z}) d\hat{z} \\
M_{gp}^{(4)} &= \int_0^\infty \mathfrak{R}_g(\hat{r}) \mathfrak{R}_p(\hat{r}) d\hat{r}; M_{hq}^{(5)} = \int_0^\infty \mathfrak{S}_h(\hat{z}) \mathfrak{S}_q(\hat{z}) d\hat{z}; M_{hq}^{(6)} = \int_0^\infty \mathfrak{S}_h(\hat{z}) \mathfrak{S}_q^*(\hat{z}) d\hat{z} \\
C_{gp}^{(4)} &= \mathfrak{W}_1 \int_0^\infty \mathfrak{R}_g(\hat{r}) \mathfrak{R}_p(\hat{r}) d\hat{r}; C_{hq}^{(5)} = \int_0^\infty \mathfrak{S}_h(\hat{z}) \mathfrak{S}_q(\hat{z}) d\hat{z}; C_{hq}^{(6)} = \int_0^\infty \mathfrak{S}_h(\hat{z}) \mathfrak{S}_q^*(\hat{z}) d\hat{z} \\
E_{gp}^{(4)} &= \mathfrak{W}_2 \int_0^\infty \mathfrak{R}_g(\hat{r}) \mathfrak{R}_p(\hat{r}) d\hat{r}; E_{hq}^{(5)} = \int_0^\infty \mathfrak{S}_h(\hat{z}) \mathfrak{S}_q''(\hat{z}) d\hat{z}; E_{hq}^{(6)} = \int_0^\infty \mathfrak{S}_h(\hat{z}) \mathfrak{S}_q''(\hat{z}) d\hat{z} \\
E_{gp}^{(7)} &= \mathfrak{W}_3 \int_0^\infty \mathfrak{R}_g(\hat{r}) \left(\mathfrak{R}_p'(\hat{r}) + \frac{1}{\hat{r}} \mathfrak{R}_p(\hat{r}) \right) d\hat{r}; E_{hq}^{(8)} = \int_0^\infty \mathfrak{S}_h(\hat{z}) \mathfrak{S}_q(\hat{z}) d\hat{z} \\
E_{hq}^{(9)} &= \int_0^\infty \mathfrak{S}_h(\hat{z}) \mathfrak{S}_q^*(\hat{z}) d\hat{z}; K_{gi}^{(7)} = \mathfrak{W}_4 \int_0^\infty \mathfrak{R}_g(\hat{r}) \left(\mathfrak{Y}_i(\hat{r}) + \frac{1}{\hat{r}} \mathfrak{Y}_i(\hat{r}) \right) d\hat{r} \\
K_{hj}^{(8)} &= \int_0^\infty \mathfrak{S}_h(\hat{z}) \mathfrak{F}_j(\hat{z}) d\hat{z}; K_{hj}^{(9)} = \int_0^\infty \mathfrak{S}_h(\hat{z}) \mathfrak{F}_j^*(\hat{z}) d\hat{z}; F_{gk}^{(3)} = \mathfrak{W}_5 \int_0^\infty \mathfrak{R}_g(\hat{r}) \psi_k(\hat{r}) d\hat{r} \\
F_{hd}^{(4)} &= \int_0^\infty \mathfrak{S}_h(\hat{z}) \Phi_d(\hat{z}) d\hat{z}; M_{ck}^{(7)} = \int_0^\infty \mathfrak{S}_c(\hat{r}) \mathfrak{S}_k(\hat{r}) d\hat{r}; M_{ld}^{(8)} = \int_0^\infty \mathfrak{L}_l(\hat{z}) \Phi_l(\hat{z}) d\hat{z}; \\
M_{ci}^{(9)} &= \mathfrak{N}_1 \int_0^\infty \mathfrak{S}_c(\hat{r}) \left(\mathfrak{Y}_i(\hat{r}) + \frac{1}{\hat{r}} \mathfrak{Y}_i(\hat{r}) \right) d\hat{r}; M_{lj}^{(10)} = \int_0^\infty \Phi_l(\hat{z}) \mathfrak{F}_j(\hat{z}) d\hat{z}; \\
M_{lj}^{(11)} &= \int_0^\infty \Phi_l(\hat{z}) \mathfrak{F}_j^*(\hat{z}) d\hat{z}; M_{cp}^{(12)} = \mathfrak{N}_1 \int_0^\infty \mathfrak{S}_c(\hat{r}) \mathfrak{R}_p(\hat{r}) d\hat{r}; \\
M_{lq}^{(13)} &= \int_0^\infty \Phi_l(\hat{z}) \mathfrak{S}_q(\hat{z}) d\hat{z}; M_{lq}^{(14)} = \int_0^\infty \Phi_l(\hat{z}) \mathfrak{S}_q^*(\hat{z}) d\hat{z}; C_{ck}^{(7)} = \mathfrak{N}_2 \int_0^\infty \mathfrak{S}_c(\hat{r}) \mathfrak{S}_k(\hat{r}) d\hat{r} \\
C_{ld}^{(8)} &= \int_0^\infty \Phi_l(\hat{z}) \Phi_d(\hat{z}) d\hat{z}; C_{ci}^{(9)} = \mathfrak{N}_3 \int_0^\infty \mathfrak{S}_c(\hat{r}) \left(\mathfrak{Y}_i(\hat{r}) + \frac{1}{\hat{r}} \mathfrak{Y}_i(\hat{r}) \right) d\hat{r}; \\
C_{lj}^{(10)} &= \int_0^\infty \Phi_l(\hat{z}) \mathfrak{F}_j(\hat{z}) d\hat{z}; C_{lj}^{(11)} = \int_0^\infty \Phi_l(\hat{z}) \mathfrak{F}_j^*(\hat{z}) d\hat{z}; C_{cp}^{(12)} = \mathfrak{N}_3 \int_0^\infty \mathfrak{S}_c(\hat{r}) \mathfrak{R}_p(\hat{r}) d\hat{r} \\
C_{cp}^{(13)} &= \int_0^\infty \mathfrak{L}_d(\hat{z}) \mathfrak{S}_q(\hat{z}) d\hat{z}; C_{cp}^{(14)} = \int_0^\infty \mathfrak{L}_d(\hat{z}) \mathfrak{S}_q^*(\hat{z}) d\hat{z}; \\
F_{ck}^{(5)} &= \int_0^\infty \mathfrak{S}_c(\hat{r}) \left(\left(\mathfrak{S}_k'(\hat{r}) + \frac{1}{\hat{r}} \mathfrak{S}_k(\hat{r}) \right) - (\mathfrak{N}_4 \mathfrak{S}_k(\hat{r})) \right) d\hat{r}; F_{ld}^{(6)} = \int_0^\infty \Phi_l(\hat{z}) \Phi_d(\hat{z}) d\hat{z}; \\
F_{ck}^{(7)} &= \int_0^\infty \mathfrak{S}_c(\hat{r}) \mathfrak{S}_k(\hat{r}) d\hat{r}; F_{ld}^{(8)} = \int_0^\infty \mathfrak{L}_l(\hat{z}) \mathfrak{L}_d(\hat{z}) d\hat{z}; \\
P_{cl}^{(1)} &= \mathfrak{N}_4 \hat{T}_b \left(\int_0^\infty \mathfrak{S}_c(\hat{r}) d\hat{r} \times \int_0^\infty \mathfrak{L}_l(\hat{z}) d\hat{z}; \right);
\end{aligned} \tag{51}$$

$$\begin{aligned}
P_{cl}^{(2)}(\hat{t}) &= \mathfrak{N}_5 \left(\int_0^\infty \mathfrak{S}_c(\hat{r}) d\hat{r} \times \int_0^\infty f_1(\hat{z}) \mathfrak{L}_l(\hat{z}) d\hat{z}; \right) \mathfrak{F}_2(\hat{t}); \\
P_{cl}^{(3)}(\hat{t}) &= \mathfrak{N}_6 \left(\int_0^\infty \mathfrak{S}_c(\hat{r}) d\hat{r} \times \int_0^\infty f_1(\hat{z}) \mathfrak{L}_l(\hat{z}) d\hat{z}; \right) \mathfrak{F}_2(\hat{t}) \\
K_{ei}^{(10)} &= \int_0^\infty \mathfrak{Y}_e(\hat{r}) \mathfrak{Y}_i(\hat{r}) d\hat{r}; K_j^{(11)} = \mathfrak{F}_j(0); K_j^{(12)} = \mathfrak{F}_j^*(0); \\
E_{ep}^{(10)} &= \int_0^\infty \mathfrak{Y}_e(\hat{r}) \mathfrak{R}_p(\hat{r}) d\hat{r}; E_q^{(11)} = \mathfrak{S}_q(0); E_q^{(12)} = \mathfrak{S}_q^*(0); \\
K_{gi}^{(13)} &= \int_0^\infty \mathfrak{R}_g(\hat{r}) \left(\mathfrak{Y}_i(\hat{r}) + \frac{1}{\hat{r}} \mathfrak{Y}_i(\hat{r}) \right) d\hat{r}; K_{gi}^{(14)} = \mathfrak{F}_j(0); K_j^{(15)} = \mathfrak{F}_j^*(0); \\
E_{gp}^{(13)} &= \mathfrak{M}_6 \int_0^\infty \mathfrak{R}_g(\hat{r}) \mathfrak{R}_p(\hat{r}) d\hat{r}; E_{gp}^{(14)} = \mathfrak{S}_q(0); E_q^{(15)} = \mathfrak{S}_q^*(0); \\
F_{gk}^{(9)} &= \mathfrak{M}_7 \int_0^\infty \mathfrak{R}_g(\hat{r}) \mathfrak{S}_k(\hat{r}) d\hat{r}; F_D^{(10)} = \mathfrak{L}_l(0)
\end{aligned}$$

The following shape functions are considered for solving the equations:

$$\begin{aligned}
\mathfrak{Y}_i(\hat{r}) &= J_l(i\hat{r}); \mathfrak{R}_p(\hat{r}) = \cos(p\pi\hat{r}) \cdot \exp(-p\hat{r}^2); \mathfrak{S}_k(\hat{r}) = e^{-k\hat{r}^2}; \mathfrak{F}_j(\hat{z}) = e^{-j\hat{z}^2} \\
\mathfrak{F}_j^*(\hat{z}) &= \hat{z} e^{-j\hat{z}^2}; \mathfrak{S}_q(\hat{z}) = e^{-q\hat{z}^2}; \mathfrak{S}_q^* = \hat{z} e^{-q\hat{z}^2}; \mathfrak{L}_d(\hat{z}) = e^{-d\hat{z}^2}
\end{aligned} \tag{52}$$

where J_l is the Bessel function of the first kind.

Considering $n = m = a = b = u = s = 1$, in equations (46-50), the parameters A and B can be obtained as:

$$\mathcal{A}_1 = \mathfrak{d}_1 \frac{\chi_{11}}{q_{11}}; \mathcal{B}_1 = \mathfrak{d}_2 \frac{q_{11}}{\chi_{11}} + \mathfrak{d}_3 \frac{\xi_{11}}{\chi_{11}} \tag{53}$$

In which α_1 , α_2 and α_3 are defined as:

$$\mathfrak{d}_1 = -\frac{E_{11}^{(10)} E_{11}^{(11)}}{K_{11}^{(10)} K_{11}^{(12)}}; \mathfrak{d}_2 = -\frac{K_{11}^{(13)} K_{11}^{(14)}}{E_{11}^{(13)} E_{11}^{(15)}}; \mathfrak{d}_3 = \frac{F_{11}^{(9)} F_{11}^{(10)}}{E_{11}^{(13)} E_{11}^{(15)}} \tag{54}$$

Substituting the parameters A and B into equations (46)-(48), they simplify to:

$$\mathcal{M}_{11}^{(1)} \ddot{q}_{11} + \mathcal{M}_{11}^{(2)} \ddot{\chi}_{11} + \mathcal{C}_{11}^{(1)} \dot{q}_{11} + \mathcal{C}_{11}^{(2)} \dot{\chi}_{11} + \mathfrak{K}_{11}^{(1)} q_{11} + \mathfrak{K}_{11}^{(2)} \chi_{11} + \mathfrak{K}_{11}^{(3)} \xi_{11} = 0 \tag{55}$$

$$\begin{aligned}
&\mathcal{M}_{11}^{(3)} \ddot{\chi}_{11} + \mathcal{M}_{11}^{(4)} \ddot{q}_{11} + \mathcal{M}_{11}^{(5)} \ddot{\xi}_{11} + \mathcal{C}_{11}^{(3)} \dot{\chi}_{11} + \mathcal{C}_{11}^{(4)} \dot{q}_{11} + \mathcal{C}_{11}^{(5)} \dot{\xi}_{11} + \mathfrak{K}_{11}^{(4)} \chi_{11} \\
&+ \mathfrak{K}_{11}^{(5)} q_{11} + \mathfrak{K}_{11}^{(6)} \xi_{11} = 0
\end{aligned} \tag{56}$$

$$\begin{aligned}
&\mathcal{M}_{11}^{(6)} \ddot{\xi}_{11} + \mathcal{M}_{11}^{(7)} \ddot{q}_{11} + \mathcal{M}_{11}^{(8)} \ddot{\chi}_{11} + \mathcal{C}_{11}^{(6)} \dot{\xi}_{11} + \mathcal{C}_{11}^{(7)} \dot{q}_{11} + \mathcal{C}_{11}^{(8)} \dot{\chi}_{11} + \mathfrak{K}_{11}^{(7)} \xi_{11} - P_{11}^{(1)} \\
&- P_{11}^{(2)} - P_{11}^{(3)} = 0
\end{aligned} \tag{57}$$

With the following coefficients:

$$\mathcal{M}_{11}^{(1)} = M_{11}^{(1)} M_{11}^{(2)}; \mathcal{M}_{11}^{(2)} = \mathfrak{d}_1 M_{11}^{(1)} M_{11}^{(3)}; \mathcal{C}_{11}^{(1)} = C_{11}^{(1)} C_{11}^{(2)}; \mathcal{C}_{11}^{(2)} = \mathfrak{d}_1 C_{11}^{(1)} C_{11}^{(3)};$$

$$\begin{aligned}
K_{11}^{(1)} &= K_{11}^{(1)} K_{11}^{(2)} + K_{11}^{(4)} K_{11}^{(5)} + d_2 E_{11}^{(1)} E_{11}^{(3)}; \\
K_{11}^{(2)} &= d_1 (K_{11}^{(1)} K_{11}^{(3)} + K_{11}^{(4)} K_{11}^{(6)}) + (E_{11}^{(1)} E_{11}^{(2)}); K_{11}^{(3)} = F_{11}^{(1)} F_{11}^{(2)} - d_3 E_{11}^{(1)} E_{11}^{(3)} \\
M_{11}^{(3)} &= M_{11}^{(4)} M_{11}^{(5)}; M_{11}^{(4)} = d_2 M_{11}^{(4)} M_{11}^{(6)}; M_{11}^{(5)} = d_3 M_{11}^{(4)} M_{11}^{(6)} \\
C_{11}^{(3)} &= C_{11}^{(4)} C_{11}^{(5)}; M_{11}^{(4)} = d_2 C_{11}^{(4)} C_{11}^{(6)}; C_{11}^{(5)} = d_3 C_{11}^{(4)} C_{11}^{(6)} \\
K_{11}^{(4)} &= (E_{11}^{(4)} E_{11}^{(5)} + E_{11}^{(7)} E_{11}^{(8)}) + d_1 K_{11}^{(7)} K_{11}^{(9)} \\
K_{11}^{(5)} &= d_2 (E_{11}^{(4)} E_{11}^{(6)} + E_{11}^{(7)} E_{11}^{(9)}) + K_{11}^{(7)} K_{11}^{(8)}; \\
K_{11}^{(6)} &= F_{11}^{(3)} F_{11}^{(3)} - d_3 (E_{11}^{(4)} E_{11}^{(6)} + E_{11}^{(7)} E_{11}^{(9)}); M_{11}^{(6)} = M_{11}^{(7)} M_{11}^{(8)} + d_3 M_{11}^{(12)} M_{11}^{(14)}; \\
M_{11}^{(7)} &= M_{11}^{(9)} M_{11}^{(10)} + d_2 M_{11}^{(12)} M_{11}^{(14)}; M_{11}^{(8)} = d_1 M_{11}^{(9)} M_{11}^{(11)} + M_{11}^{(12)} M_{11}^{(13)}; \\
C_{11}^{(6)} &= C_{11}^{(7)} C_{11}^{(8)} + d_3 C_{11}^{(12)} C_{11}^{(14)}; C_{11}^{(7)} = C_{11}^{(9)} C_{11}^{(10)} + d_2 C_{11}^{(12)} C_{11}^{(14)}; \\
C_{11}^{(8)} &= C_{11}^{(12)} C_{11}^{(13)} + d_1 C_{11}^{(9)} C_{11}^{(11)}; K_{11}^{(7)} = F_{11}^{(5)} F_{11}^{(6)} + F_{11}^{(7)} F_{11}^{(8)}
\end{aligned} \tag{58}$$

Equations (55-57) are solved simultaneously to obtain the transient temperature and vibration response of the skin tissue.

4. Numerical Results

For numerical calculation, values of heat and physical properties of skin tissue, blood, and the parameters of the laser heat source are listed in Table 1.

Table 1 Properties of skin tissue and the laser heat source [25,45]

Density of tissue (ρ)	1000 (kg/m^3)
Density of blood (ρ_b)	1060 (kg/m^3)
Specific heat of the tissue (c)	4187 ($J/kg.K$)
Specific heat of blood (c_b)	3860 ($J/kg.K$)
Heat conductivity of tissue (k)	0.628 ($W/m.K$)
Blood perfusion (G_b)	1.87E-3 ($1/s$)
Relaxation time (τ)	3 (s)
Elasticity modulus of tissue (E)	100 (MPa)
Thermal expansion (α_T)	1E-4 ($1/K$)
Poisson's ratio (ν)	0.4
Laser intensity (I_0)	3E+5 (W/m^2)
Diffuse reflectance (R_d)	0.05
Reference temperature (T_0)	37 0C

In this section, the transient thermomechanical response of skin tissue subjected to different types of heating sources is investigated.

4.1 Single-pulse heating source

Considering the single pulse heating source shown in Figure 2a, the temperature response of skin tissue is presented and shown in Figure 2b.

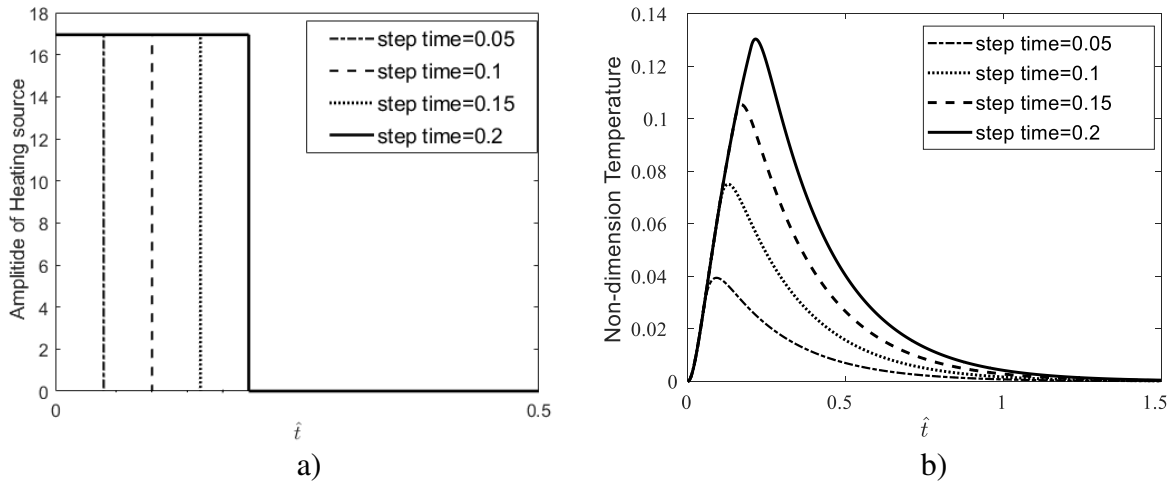


Figure 2a) Single-pulse heating source b) Temperature response of skin tissue to a single-pulse heat source with different step times

The results indicate that in a laser single pulse heating source with high step time, the tissue can reach higher temperatures than a heating source with low step time. It is also observed that the step time does not affect the gradient of temperature in the heating process but increases the temperature gradient in the cooling process. The displacement response of tissue in the depth direction (z-direction) is shown in Figure 3a, and in Figure 3b, it is compared to the displacement response of tissue in the radial direction (r-direction).

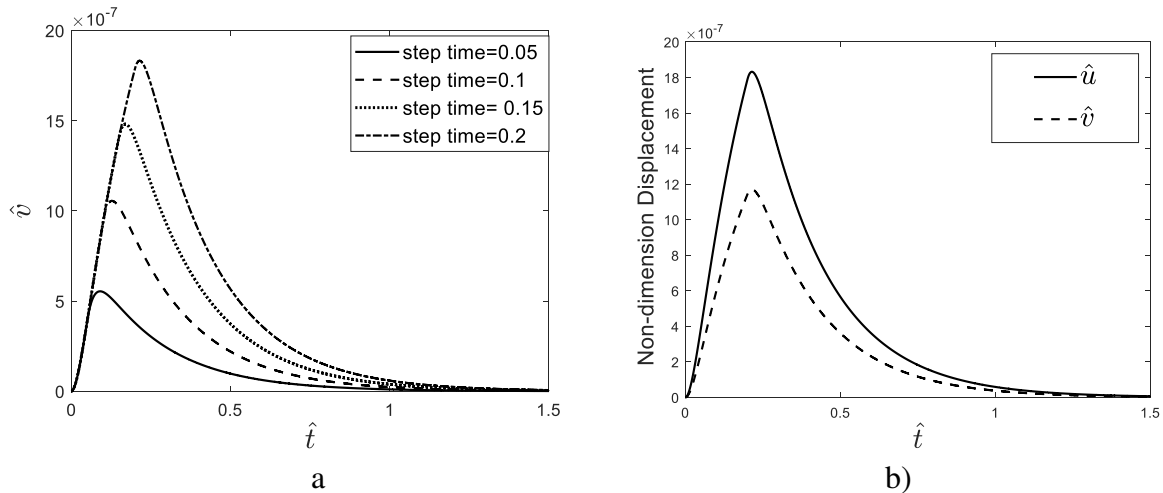


Figure 3a) Displacement response of skin tissue in the z-direction to a single-pulse heat source with different step times. b) Comparison of the displacement response of skin tissue in the depth direction with its response in the radial direction

A higher step time increases the maximum displacement of the tissue and reaches the maximum temperature. It also increases the displacement gradient of tissue in the cooling process, while it does not affect the gradient of displacement in the heating process. Figure 4 shows the temperature

of skin tissue versus time considering different values of relaxation time. It was mentioned that in the generalized Fourier law, an inertial term is considered for the heat transfer phenomenon, which is concerned with the relaxation time. An increase in the relaxation time leads to an increase in the inertial effects and therefore causes the reached maximum temperature to decrease.

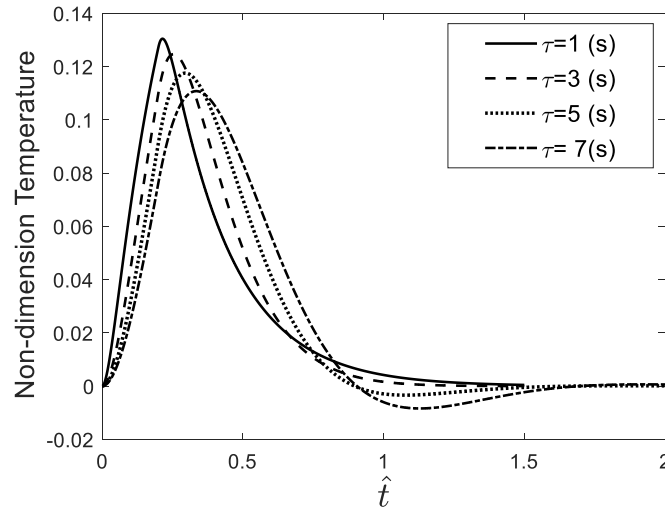


Figure 4 Temperature response of the skin tissue considering different relaxation time values

4.2 Repetitive pulse heating source

Considering the repetitive pulse heating source shown in Figure 5a, the displacement response of skin tissue is shown in Figure 5b. The results indicate that increasing relaxation time decreases the temperature gradient at the beginning of the heating process. In other words, relaxation time decreases the first maximum overshoot and increases the pick time in the response of the skin tissue. Relaxation time also reduces the amplitude of temperature vibrations of the skin in the whole heating process.

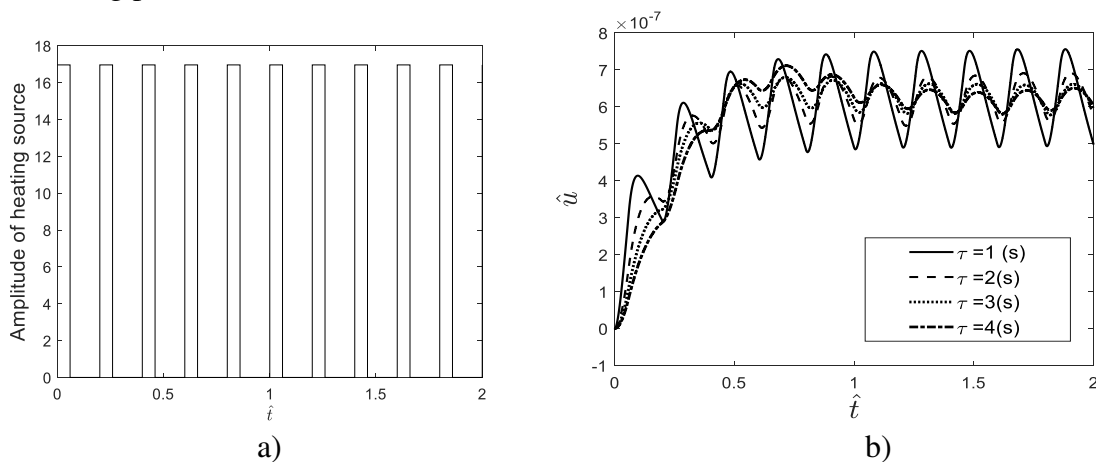


Figure 5a) Repetitive pulse heating source, b) Displacement response of skin tissue considering different relaxation times

The effect of the period and width of the repetitive pulses on the thermomechanical response of the tissue was investigated. The indicated results in Figure 6a and Figure 6b show that when the period of the pulses reduces, the amplitude of temperature vibrations decreases; therefore, the temperature response of tissue will be similar to the response subjected to the step heating source. Moreover, by increasing the width of laser pulses, the tissue can reach high temperatures during the heating process.

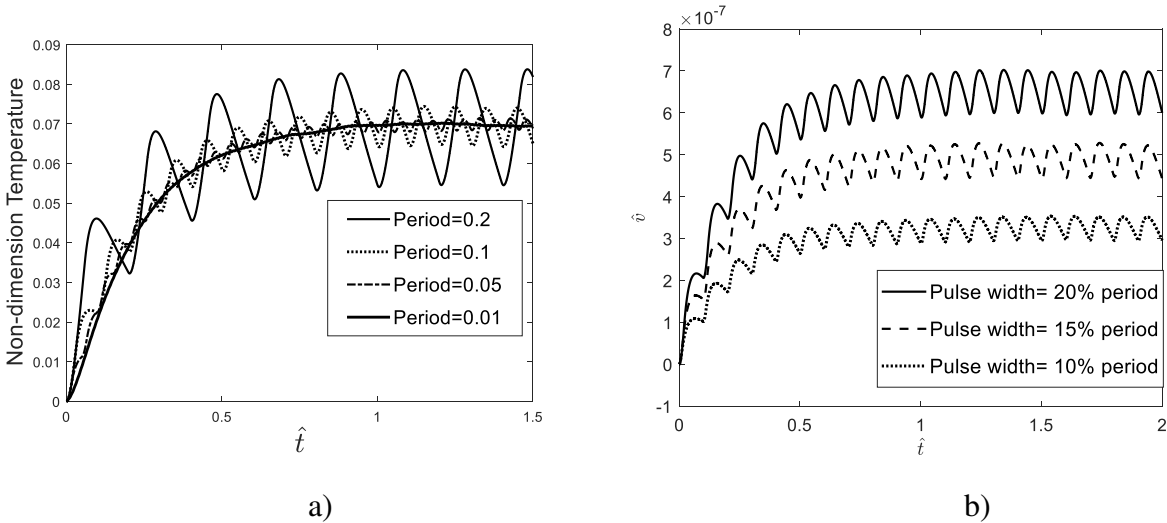


Figure 6a) The effect of the period b) The effect of the width of the repetitive pulses on the thermomechanical response of the tissue.

4.3 Repeating sequence stair

Different types of repeating sequence stair heating sources are shown in Figure 7a, 7b, and 7c. In Figure 7a, the sequence stairs are applied in the cooling stage. In Figure 7b, the sequence stairs are applied in the heating stage, and in Figure 7c, symmetric sequence stairs are applied in the heating and cooling stages of skin heating. The nondimensional temperature of skin tissue versus time is shown in Figure 7d). When sequence stairs are applied in the heating stage, the tissue can experience a higher maximum temperature than when they are applied in the cooling stage. In other words, heating the skin gradually by sequence stairs and cooling it suddenly, tissue can experience higher temperature rise compared to the case when it is heated suddenly and cooled gradually. When a symmetric sequence stairs heating source is applied to the skin, the temperature rise is low compared with two other cases.

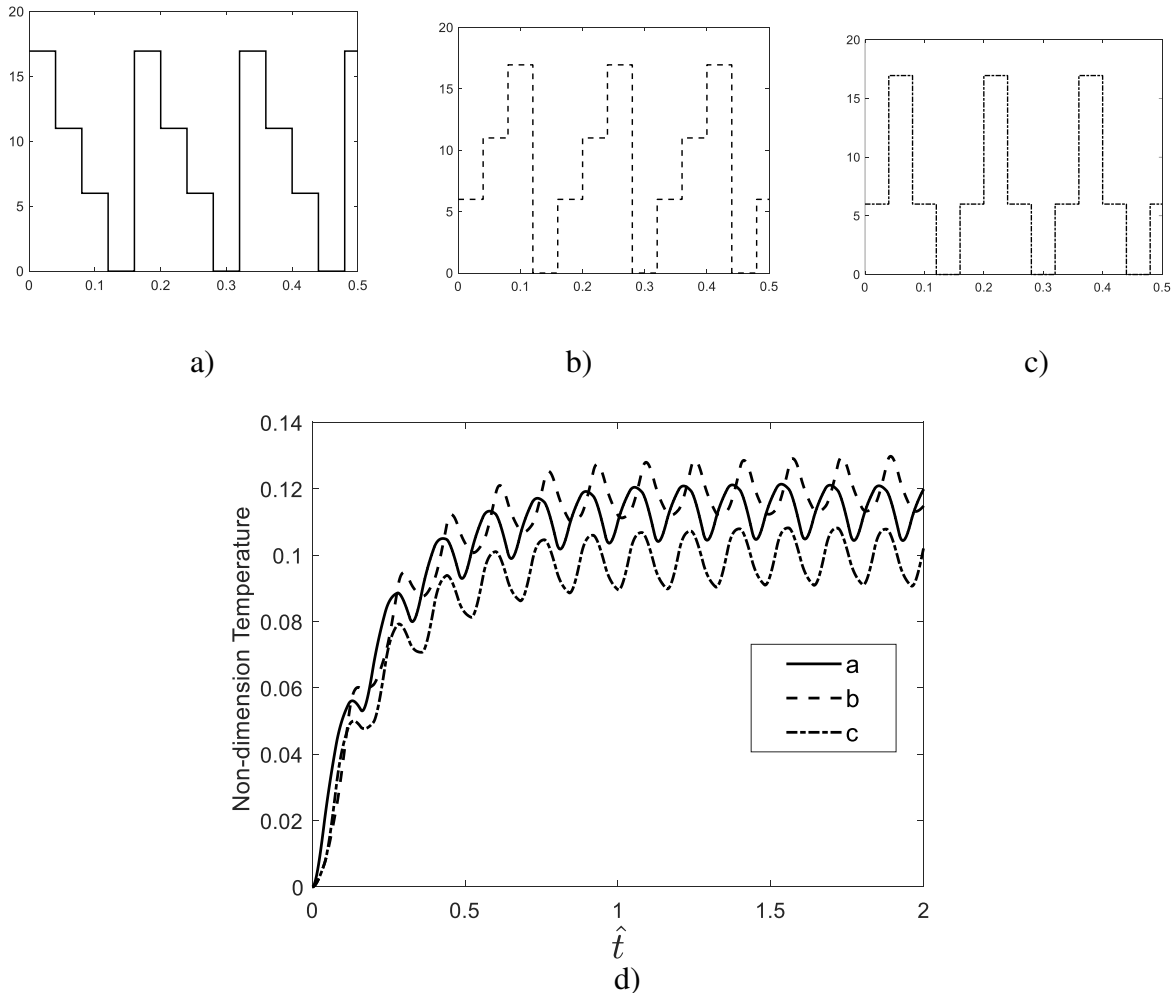


Figure 7a), 7b), 7c) Different types of repeating sequence stairs, d) Nondimensional temperature of tissue versus time considering different types of repeating sequence stairs heating sources

4.4 Step heating source

Figure 8 shows the temperature response of the skin tissue, considering a step heating source. At very low relaxation times, the skin tissue does not experience any overshoot in the thermal response. Increasing the relaxation time may lead the tissue to encounter an overshoot during its transient response. The nondimensional displacement of tissue along the z-direction at $\hat{t} = 0.1$ for different values of \hat{r} is shown in Figure 9a and Figure 9b. The results indicate that by moving away from the center of the tissue where the pulse heating source is applied, the displacement of tissue in the r- and z-directions decreases and eventually vanishes.

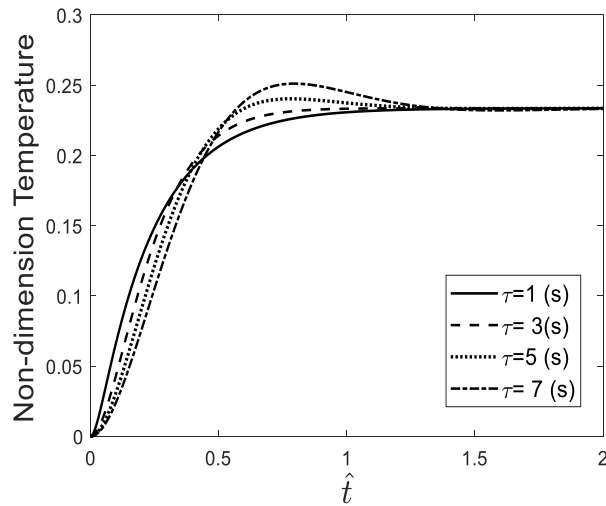


Figure 8 Temperature response of skin tissue considering the step heating source

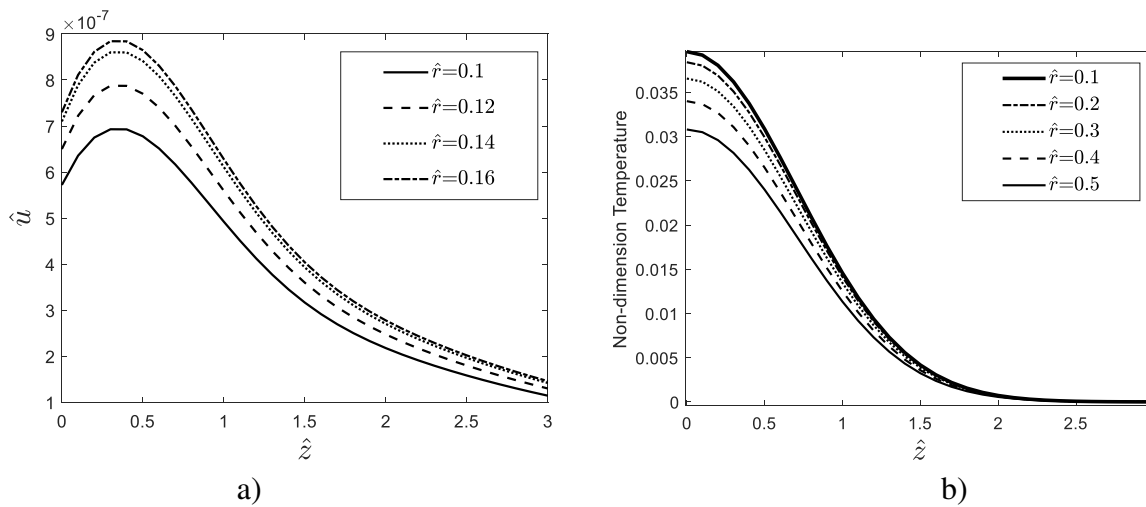


Figure 9a) Nondimensional displacement of tissue through the z-direction versus \hat{z} at $\hat{t} = 0.1$ for different values of \hat{r} and b) temperature distribution through the z-direction at $\hat{t} = 0.1$ for different values of \hat{r}

4.5 Repetitive ramp heating source

Figure 10a) shows the respective ramp heating source with different repeating times, and Figure 10b) represents the transient response of the tissue. Reducing the repeating time decreases the vibrating amplitude of temperature, therefore causing the skin to experience a low-temperature rise.

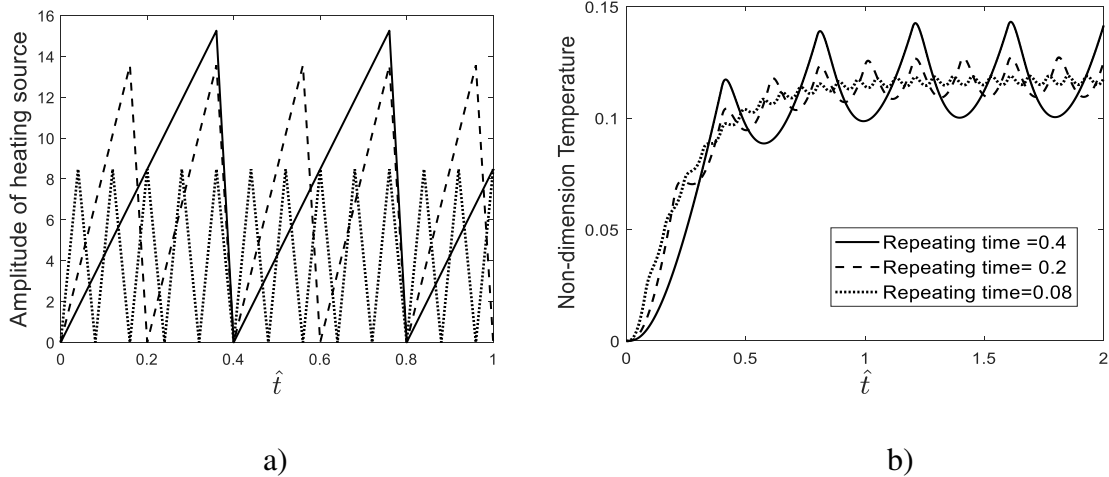


Figure 10a) Repetitive ramp heating source, b) temperature response of skin tissue considering different repeating times

4.6 Harmonic heating source

The transient thermal response of skin tissue is studied supposing a harmonic heating source. Figure 11 shows the temperature response of tissue to the harmonic heating source considering different value frequency ratios (ω_r). The frequency ratio is defined as the ratio of the excitation frequency to the characteristic frequency of the tissue ($\frac{\alpha}{h^2}$). The frequency ratio displaces the time at which the tissue reaches the maximum temperature.

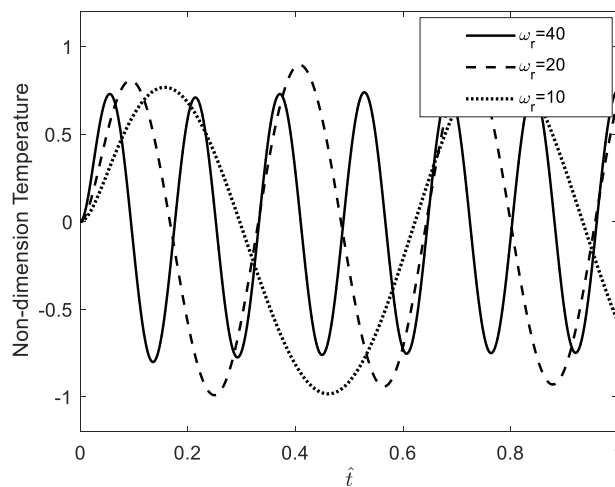


Figure 11 Temperature response of skin tissue to different frequency ratios

5. Conclusion

In the present study, the thermomechanical behavior of skin tissue exposed to different types of heating sources was presented. 2-D coupled differential equations of the hyperbolic heat transfer and 2-D dynamic displacement of tissue were extracted, considering the thermoelastic coupling term. The mixed accompanying boundary conditions (displacement and force) governing the displacement equation that have made the solution of the equations so complicated were imposed using a heuristic method. A Galerkin-based reduced-order model was utilized to solve the coupled equations with mixed boundary conditions. The transient temperature and displacement response of the tissue were analyzed under different types of thermal heating loading. It was shown that when a single pulse heating source with a high step time is applied on the skin, the tissue experiences a higher temperature rise. No changes in the temperature gradient were observed in the heating stage of the process. However, the temperature gradient in the cooling process was increased. In the case of repetitive pulses, a decrease in the period of the pulses led to a reduction in the amplitude of the temperature vibrations. It was observed that when a sequence stair is applied in the cooling stage, the tissue can reach a higher maximum temperature compared with the case when it is applied in the heating stage. Increasing the relaxation time in the step thermal loading caused the tissue to experience an overshoot during its transient response. Reducing the repeating time in the ramp-type heating source decreased the amplitude of the temperature vibration.

The authors have no conflict of interest to declare

References

- [1] Habash RW, Bansal R, Krewski D, Alhafid HT. 2006. Thermal therapy, part 1: An introduction to thermal therapy. *Critical Reviews in Biomedical Engineering*, 34(6):459-89.
- [2] Ashraf O, Patel NV, Hanft S, Danish SF. 2018. Laser-Induced Thermal Therapy in Neuro-Oncology: A Review. *World Neurosurg.* Apr;112:166-177
- [3] Stafford RJ, Fuentes D, Elliott AA, Weinberg JS, Ahrar K. 2010. Laser-induced thermal therapy for tumor ablation *Critical Reviews in Biomedical Engineering*, 38(1):79-100
- [4] Riordan M, Tovar-Spinoza Z. 2014. Laser-induced thermal therapy (LITT) for pediatric brain tumors: case-based review, *Translational Pediatrics*, 3(3):229-235
- [5] van Esser S. V, Stapper G, van Diest P. J, van den Bosch M.A.A. J, Klaessens J.H.G. M et al. 2009. Ultrasound-guided laser-induced thermal therapy for small palpable invasive breast carcinomas: A feasibility study, *Annals of Surgical Oncology* 16(8): 2259-2263
- [6] Tierney EP, Eisen RF, Hanke CW. 2011. Fractionated CO₂ laser skin rejuvenation. *Dermatologic Therapy*,24(1):41–53.
- [7] Ross EV, Miller C, Meehan K, McKinlay J, Sajben P, Trafeli JP, Barnette DJ. 2001. One-pass CO₂ versus multiple-pass Er:YAG laser resurfacing in the treatment of rhytides: A comparison side-by-side study of pulsed CO₂ and Er:YAG lasers. *Dermatologic Surgery*, 27(8):709–715
- [8] Zachary CB. Modulating the Er:YAG laser. 2000. *Lasers in Surgery and Medicine*, 26(2):223–226
- [9] Kokolakis G, von Eichel L, Ulrich M, Lademann J, Zuberbier T, Hofmann MA. 2019. Kinetics and tissue repair process following fractional bipolar radiofrequency treatment. *Journal of Cosmetic and Laser Therapy*, 21(2):71–75.
- [10] Vachiramon V, Jurairattanaporn N, Harnchoowong S, Chayavichitsilp P. 2018. Non-invasive high-intensity focused ultrasound for UV-induced hyperpigmentation in Fitzpatrick skin types III

and IV: A prospective, randomized, controlled, evaluator-blinded trial. *Lasers in Medical Science*, 33(2):361–367

[11] Elman M, Fournier N, Barneon G, Bernstein EF, Lask G. 2016. Fractional treatment of aging skin with Tixel, a clinical and histological evaluation. *Journal of cosmetic and Cosmet Laser Therapy*, 18(1): 31–37

[12] Sintov AC, Hofmann MA. 2016. A novel thermo-mechanical system enhanced transdermal delivery of hydrophilic active agents by fractional ablation. *International Journal of Pharmaceutics*, 511(2):821–830.

[13] Kokolakis G, Grawert LV, Ulrich M, Lademann J, Zuberbier T, Hofmann MA. 2020. Wound healing process after thermomechanical skin ablation, *Lasers in Surgery and Medicine*, 52(8):788-798

[14] Ha L, Jaspán M, Welford D, Evers M, Kosiratna G, Casper M.J, Manstein D, Birngruber R. 2020. First assessment of a carbon monoxide laser and a thulium fiber laser for fractional ablation of skin, *Lasers in Surgery and Medicine*, 52(8):788-798

[15] Kisilevitz M, Lu K.B, Wamsley M, Hoopman J, Kenkel J, Akgul Y. 2019. Novel use of noninvasive devices and microbiopsies to assess facial skin rejuvenation following laser treatment, *Lasers in Surgery and Medicine*, 52(9): 822-830

[16] Pennes H.H. 1948. Analysis of Tissue and Arterial Blood Temperatures in the Resting Forearm, *Journal of Applied Physiology* 1:93-122

[17] Chen M.M, and Holmes K.R. 1980. Microvascular Contributions in Tissue Heat Transfer, *Annals of the New York Academy of Sciences*, 335: 137-150, 1980.

[18] Jiji, L.M., Weinbaum, S., and Lemons, D.E. 1984. Theory and Experiment for the Effect of Vascular Microstructure on Surface tissue Heat Transfer-Part II: Model Formulation and Solution,” *ASME J. of Biomechanical Engineering*, 106:331-341

[19] Weinbaum, S., and Jiji, L.M., “A New Simplified Bioheat Equation for the Effect of Blood Flow on Local Average Tissue Temperature,” *ASME J. of Biomechanical Engineering*, 107: 131-139, 1985

[20] Cattaneo C. 1958. A form of heat conduction equation which eliminates the paradox of instantaneous propagation, *C. R. Acad. Bulg. Sci.: Sciences Mathematiques et Naturelles* 247:431–433.

[21] Vernotte P. 1958. Les paradoxes de la theorie continue de l’equation de la chaleur, *C. R. Acad. Bulg. Sci.: Sciences Mathematiques et Naturelles*, 246: 3154–3155.

[22] Zisik M. N., Tzou D. Y. On the wave theory in heat conduction. *Journal of Heat Transfer*, Vol. 116, 1994, p. 526-535.

[23] Tzou D.Y. 1995. The generalized lagging response in small-scale and high-rate heating, *International Journal of Heat and Mass Transfer*, 38 (17): 3231–3240.

[24] Tzou D. Y. 1995. A unified field approach for heat conduction from macro- to microscales, *Journal of Heat Transfer-transactions of The ASME*. 117 (1): 8–16.

[25] Alzahrani A, Abbas I.A. 2019. Analytical estimations of temperature in a living tissue generated by laser irradiation using experimental data, *Journal of Thermal Biology*, 85:102421

[26] Zhang Y, Chen B, Li Dong. 2017. Non-Fourier effect of laser-mediated thermal behaviors in biotissues: A numerical study by the dual-phase-lag model, *International Journal of Heat and Mass Transfer* 108:1428-1438

[27] Mondal S, Sur Abhik, Kanoria M. 2021. Transient heating within skin tissue due to time-dependent thermal therapy in the context of memory dependent heat transport law, *Mechanics Based Design of Structures and Machines*, 49(2): 271-285

- [28] Zhang Q, Sun Y, Yang J, Soh A.K, Wang X. 2021. Theoretical analysis of thermal response in biological skin tissue subjected to multiple laser beams, *Case Studies in Thermal Engineering*, 24:100853
- [29] Liu K.C, Chen H.T. 2010. Investigation for the dual phase lag behavior of bioheat transfer, *International Journal of Thermal Sciences*, 49:1138-1146
- [30] Li x, Li C, Xue Z, Tian x. 2018. Analytical study of transient thermomechanical responses of dual-layer skin tissue with variable thermal material properties, *International Journal of Thermal Sciences*, 124:459-466
- [31] Liu K.C, Chen H.T. 2009. Analysis for the dual-phase-lag bioheat transfer during magnetic hyperthermia treatment, *International Journal of Heat and Mass Transfer*, 52:1185-1192
- [32] Ma J, Yang X, Sun Y, Yang J. 2021. Theoretical analysis on thermal treatment of skin with repetitive pulses, *Scientific reports*, 11, 9958
- [33] Wang Y.Z, Li M.J, Liu D. 2021. Thermomechanical interaction on transient heating of skin tissue with variable thermal material properties, *European Journal of Mechanics -A/Solid*, 86:104173
- [34] Ezzat M.A. 2021. Analytical study of two-dimensional thermomechanical responses of viscoelastic skin tissue with temperature-dependent thermal conductivity and rheological properties, *Mechanics Based Design of Structures and Machines*,
- [352] Gao F, Feng X, Zheng Y .2015. Photoacoustic elastic oscillation and characterization, *Optics Express* 23(16):20617-28 <https://doi.org/10.1364/OE.23.020617>
- [36] Gao F, Feng X, Zheng Y, Ohl C.D. 2014. Photoacoustic resonance spectroscopy for biological tissue characterization, *Journal of Biomedical Optics*, 19(6):067006
- [37] Boley B.A. 1972. Survey of recent developments in the fields of heat conduction in solids and thermoelasticity, *Nuclear Engineering and Design*, 18(3):377–399 3,
- [38] Wang Y, Liu D, Wang Q, Shu C.2015. Thermoelastic response of thin plate with variable material properties under transient thermal shock, *International Journal of Mechanical Sciences*, 104(Supplement C):200–206
- [39] Yussef H.M, Alghamdi N.A. 2020. Modeling of one-dimensional thermoelastic dual-phase lag skin tissue subjected to different types of thermal loading, *Scientific reports*, 10:3399
- [40] Entezari A, Filippi M, Carrera E, Kouchakzadeh M.A.2018. 3D dynamic coupled thermoelastic solution for constant thickness disks using refined 1D finite element models. *Applied Mathematical Modeling*, 60:273–285
- [41] Tsai T. W, Lee Y.M. 2013. Analysis of microscale heat transfer and ultrafast thermoelasticity in a multilayered metal film with nonlinear thermal boundary resistance. *International Journal of Heat and Mass Transfer*, 62:87–98
- [42] Zener C. 1938., Internal friction in solids. II. General theory of thermoelastic internal friction, *Physics Review*,53:90-99.
- [43] Rezaazadeh G, Vahdat A.S, Pesteii S.M. Farzi B. 2009. Study of thermoelastic damping in capacitive microbeam resonator using hyperbolic heat conduction model, *Sensors and Transducers*, 108(9): 54-72
- [44] Zamani A, Eslami M.R. 2010. Implementation of the extended finite element method for dynamic thermoelastic fracture initiation. *International Journal of Solids and Structures*, 47(10):1392–1404
- [45] Xu F, Lu T. J, Seffen K.A. 2008. Biothermomechanical behavior of skin tissue. *Acta Mechanica Sinica*, 24:1-23